An investigation into the effects of outer membrane vesicles and Lipopolysaccharide (LPS) of *Porphyromonas gingivalis* on blood brain barrier integrity, permeability and disruption of scaffolding proteins in a human in vitro model.

Anna Barlach **Pritchard** [a], Zsolt **Fabian** [b], Clare L **Lawrence** [c], Glyn **Morton** [d], StJohn **Crean** [a] and Jane E **Alder** [c]

[a] Brain and Behaviour Centre, Faculty of Clinical and Biomedical Sciences, School of Dentistry, University of Central Lancashire, Preston, UK.

[b] School of Medicine, University of Central Lancashire, Preston, UK

[c] Brain and Behaviour Centre, Faculty of Clinical and Biomedical Sciences, School of Pharmacy and Biomedical Sciences, University of Central Lancashire, Preston, UK.

[d] School of Forensic and Investigative Science, University of Central Lancashire, Preston, UK

*Correspondence to Anna Barlach Pritchard, Brain and Behaviour Centre, Faculty of Clinical and Biomedical Sciences, School of Dentistry, University of Central Lancashire, Preston, UK. Tel.: +44 0 1772 895906; E-mail: abpritchard@uclan.ac.uk

ABSTRACT

The journey and effects of gum disease key pathogens such as *Porphyromonas gingivalis* (*P.gingivalis*) and its virulence factors to and on the central nervous system is of great interest with respect to development of therapeutics and preventative strategies. The role of chronic infections and associated inflammation is important as both are known to weaken the first line of defence for the brain; the blood brain barrier (BBB). The focus of this study is to utilise an established human *in vitro* BBB model to evaluate the effects of *P.gingivalis* virulence factors Lipopolysaccharide (LPS) and outer membrane vesicles (OMVs) on a primary-derived human model representing the neuro vascular unit of the BBB. Changes to the integrity of the BBB after application of *P.gingivalis* LPS and OMVs were investigated and correlated with transport of LPS . Additionally, the effect of *P.gingivalis* LPS and OMVs on human brain microvascular endothelial cells in monolayer was evaluated using immunofluorescence microscopy. The integrity of the BBB model was weakened by application of *P.gingivalis* LPS and OMVs, as measured by a decrease in electrical resistance (TEER) and a recovery deficit was seen in comparison to the controls. Application of *P.gingivalis* OMVs to a monoculture of human brain microvascular endothelial cells (HBMEC) showed disruption of the tight junction zona occludens protein (ZO-1) compared to controls. These findings show that the integrity of healthy cells and potentially their tight junctions of the human BBB could be weakened by association with *P.gingivalis* virulence factors LPS and OMVs containing proteolytic enzymes (gingipains).

Keywords

Blood brain barrier, HBMEC, Alzheimer's Disease, micro biome, Periodontal disease, *in vitro* BBB model.

BACKGROUND

The concept of a microbial cause or risk factor for neurodegenerating disease such as sporadic Alzheimer's Disease has gathered momentum in the past decade. Why some individuals develop sporadic Alzheimer's Disease (AD) while others are resistant remains unresolved. There is currently no effective treatment for AD or a way of slowing or stopping the rate of neurodegeneration. What has emerged is a body of evidence over the past decade which supports a possible microbial role in the development of neurodegeneration, which includes epidemiological data, post-mortem and experimental studies. The evidence suggests that microbials potentially linked to AD may be viral, bacterial or fungal in origin [1,2,3,4]. It is known that there are multiple risk factors for developing sporadic AD, the most significant being advanced age [4]. However, the possibility of a microbial role as a causative factor for AD, opens new possibilities for the discovery of novel preventative measures and therapeutic targets. Pivotal to the discovery of such novel drug targets is the need to create research models that are representative of human physiology and disease state.

AD is a chronic neurodegenerative condition which is known to develop over decades, displaying histological hallmarks of extracellular amyloid-β (Aβ) plaques and hyper phosphorylated intracellular Tau tangles within the brain parenchyma [5]. AD can also be considered as a chronic inflammatory disease and has been linked to inflammatory events [6] such as traumatic brain injury or vascular disease, with subsequent activation of the immune system and release of appropriate inflammatory mediators purposely to protect the brain. If an individual predisposed either through age, genetics, illness or lifestyle habits (smoking, diet, exercise) [7],

develops a persistent inflammatory trigger, then this can establish a chronic tissue reaction with devastating toxic effects at a cellular level [8] and even initiating a path to recognised AD pathology [6]. Sporadic AD presents late in life in individuals who may not have an overt history of an acute inflammatory event, but the pathological end point is the same [8]. The search for a trigger of raised levels of pro-inflammatory mediators and oxidative stress, identified in AD patients goes on.

The detection of multiple microbials in post-mortem brains from AD individuals and the notion that Aβ can behave as an anti-microbial peptide [9,10] raises the possibility that an external [chronic] assault on brain tissues, for example infection by the oral periodontal disease bacteria *Porphyromonas gingivalis* (*P.gingivalis*), could cumulatively damage brain tissue and even lead to low level neurodegenerative changes decades before a clinical diagnosis of AD presents [8].

Periodontal disease (PD) is a chronic infection caused by bacteria in the gums around teeth represented by microbial dysbiosis and tissue destruction [11,12]. PD has been linked to other organ specific disease such as Alzheimer's Disease, atherosclerosis, and diabetes mellitus [13,14]. The progression of PD in humans is determined by microbiological, environmental and genetic factors (multiple polymorphisms) [15]. It can go undiagnosed for years and even if oral hygiene measures are improved, there is a potential of daily bacteraemia (s) of periodontal pathogens when chewing foods or cleaning teeth [16]. It is this chronic bacterial load in the circulation which is proposed to contribute to a systemic chronic inflammatory state.

P.gingivalis, an anaerobic Gram-negative coccobacillus, is a key pathogen of PD and has numerous mechanisms which can affect the surroundings tissues including i) endotoxin or lipopolysaccharide (LPS) mainly located on the outer membrane and ii) via release of outer membrane vesicles (OMVs) by the Type IX secretion system. The

working hypothesis the authors propose is that a chronic assault on the BBB from circulating periodontal pathogens and/or their associated virulence factors could lead to disruption of the integrity of the barrier (either by increased permeability or reduction in clearance). Whilst there is some evidence to support the concept it remains incompletely evidenced in humans and *P.gingivalis* cells have not yet been found in the brain of AD patients or test animals[13]. However, human post-mortem studies have found evidence of *P.gingivalis* DNA and virulence factors, LPS and proteases secreted by *P.gingivalis* (gingipains), in the brains of AD individuals [17,18]. *In vivo* animal studies, investigating the administration of *P.gingivalis* associated virulence factors have shown that these substances travel to and settle in the animal's brain [19,20]. Illievski et al., (2018) [20] showed that infection of mice with *P.gingivalis induced* neuroinflammation and appeared to induce the deposition of intracerebral Aβ protein, drawing similarities to the human AD pathology. It remains unclear however, whether the reason for the Aβ protein seen in the brain of the test animals was due to a direct cerebral invasion of intact *P.gingivalis*, its virulence factors such as gingipains or an indirect effect from the inflammatory mediators of systemic infection [20]. The authors suggest two pathways for *P.gingivalis* inducing neurodegenerative changes. Either i) *P.gingivalis* can access the brain directly or ii) the bacteria can orchestrate the neurological changes from a distant site of infection, i.e., the periodontal pockets in the oral cavity. The key question remains if or how *P.gingivalis* and its virulence factors access brain tissue, how do they cross the BBB?

P.GINGIVALIS AND ASSOCIATED VIRULENCE FACTORS

The virulence or invasive ability of a *P.gingivalis* strain can be classified according to the expression of fimbriae, capsule, LPS and gingipains release [21]. These virulence

122 factors originate from the mother cell but are disseminated wider by release of
123 OMVs. As an example, the non-capsulated laboratory strain FDC 381 has been
124 shown to invade carcinoma cells 10^3 times more than other *P.gingivalis* strains [21],
125 though FDC 381 is classed as a less virulent type causing only mild localised
126 abscesses [22]. These findings highlight two key aspects of *P.gingivalis* behaviour
127 which have significance for pathological development, the ability of the bacterium to
128 i) invade tissues and ii) modulate the subsequent immune response of the host.
129 Furthermore, a variance between different invasive abilities of OMVs from
130 *P.gingivalis* strains has been attributed to the expression of long fimbriae (not FimA)
131 and the gingipain adhesive domains in the outer membrane [23]. OMVs of
132 *P.gingivalis* are highly enriched in the proteolytic gingipains (RgpA/B and Kgp) and
133 the nano sized spheres also incorporate high concentrations of LPS and fimbriae [24]
134 which are sustainable in human tissues such as the brain [25]. *P.gingivalis* OMVs,
135 containing a high concentration of enzymes, are considered to have both harmful
136 and beneficial roles, enabling *P.gingivalis* to regulate its microenvironment [26].
137 Internalised OMVs are associated with cell degradation [27] and induction of an
138 innate immune response with a greater intensity than initiated by the bacteria itself.
139 Gingipains are also believed to help *P.gingivalis* evade the reach of the immune
140 system, making *P.gingivalis* so successful in establishing a chronic diseased state
141 [28].

142 *P.gingivalis* has also been shown to dysregulate dendritic cells by disturbing their
143 ability toward autophagy and apoptosis [29] endowing this pathogen with an
144 exceptional ability for self-preservation. Labelled *P.gingivalis* OMVs have also been
145 shown to be taken up by cortical microglial cells in mice, 24 -48 hours after
146 peripheral injection highlighting the potential reach of this virulence factor. It has
147 even been suggested that OMVs may act as a decoy to the host immune system,

diverting attention and thus protecting the mother cell from elimination [30], forming another element of *P.gingivalis'* immune evasive strategy. The size and proteolytic capacity of the OMVs makes the spread into tissues easier than for the intact bacteria and OMVs are more likely to survive transport to remote organs.

LPS from the outer membrane of Gram-negative bacteria is a powerful pro-inflammatory pathogen associated molecular pattern (PAMP) and previous studies support the capabilities of oral bacterial LPS as an inducer of peripheral inflammatory responses and as an initiating factor in intracerebral inflammatory activity [17,20]. The LPS of *P.gingivalis* has been extensively studied in relation to its pathogenicity, is found in both a soluble and membrane bound form and binds to TLR4 enhanced by sCD14 [31] activating pro-inflammatory pathways.

HUMAN BLOOD BRAIN BARRIER

The cells of the blood brain barrier, also described as the neuro vascular unit (NVU), comprise of endothelial cells, pericytes, astrocytes and neurons [32]. The 400 miles of capillaries in the human brain [33] makes this the largest potential entry point for pathogens to the CNS, but its intimate integrity affords a significant barrier. This integrity arises from; endothelial cell i) intercellular tight junctions displaying high electrical resistance, limiting any transcytosis compared to peripheral endothelial cells [34], ii) lack of fenestrae (transcellular pores) and iii) shared basement membrane with pericytes with reduced pinocytic activity. Human *in vitro* BBB models are used to investigate both disease and drug interactions of this interface providing a very valuable tool to assess permeability, transport and transendothelial electrical resistance (TEER), as well as expression of proteins [35]. The benefits of using a human primary-derived cell-based model are numerous and combinations of

cells of the NVU have been validated and standardised, for a comprehensive review see [35].

The integrity of the BBB is reduced naturally as we age [36] and multiple neurological conditions have been associated with a "leaky" BBB [34], including AD and Parkinson's disease, implying the importance its role in brain homeostasis and risk of age-related neurodegeneration [13]. Many of these neurological conditions also present with a raised level of systemic pro-inflammatory cytokines which are also thought capable of contributing to weakening in the barrier's integument [37,38].

Studies in mouse apolipoprotein E (ApoE) knock-out models [39] and humans who express the E4 isoform of (APOE4), the most prevalent predisposed genetic risk factor for AD, also show accelerated breakdown of the BBB structure and degeneration of brain capillary pericytes required for barrier integrity [40].

CNS PERMEATION BY P.GINGIVALIS AND ASSOCIATED VIRULENCE FACTORS

The journey for *P.gingivalis* and associated virulence factors, from the periodontal pocket to the central nervous system (CNS) has been suggested to follow a number of possible routes, such as tracking along the trigeminal or olfactory nerves [41], by being internalised by peripheral immune cells and subsequently transferring to the CNS or finally arriving in the systemic circulation at the BBB or the blood cerebrospinal fluid barrier (BCSFB) [42].

Both Gram negative and positive bacteria can cross at the BBB and BCSFB interfaces to the CNS by transcytosis. Bacteria such as *Neisseria.meningitidis* are able to open endothelial intercellular junctions to cross the CNS barriers in acute infection [42]

and *P.gingivalis* gingipains have been shown to degrade the epithelial JAM-1 protein [43] and induce cell adhesion molecule cleavage and apoptosis in human microvascular endothelial cells [44]. *P.gingivalis* has also been demonstrated to induce apoptosis and tight junction disruption in cultured human lung epithelial cells [45]. It is not clear however, whether these findings were caused by the bacteria or its virulence factors.

NEUROINFLAMMATION

If *P.gingivalis* was shown to induce damage to the BBB of an individual, some time before any neuroinflammation becomes clinically detectable, then the authors propose that bacteria or associated virulence factors must be capable of damaging the BBB enough to trigger a change either to its integrity allowing an influx of inflammagens and/or weakening the barrier's normal clearance strategies. If the initial causal factor for the pro-inflammatory state is not resolved, then any subsequent effects of chronic oxidative stress on the NVU cells can lead to loss of redox balance, alterations in numbers and differentiation of T-cells subpopulations and subsequent loss of regulation of the neuroinflammatory response [46]. Animal studies for example have demonstrated that LPS can incite oxidative stress, activation of glial cells and tight junction degradation in the NVU and surrounding cells [47,48].

Though much research has been undertaken to understand the events at the BBB in diseased individuals [47,48,49] and the effects of *P.gingivalis* and its virulence factors on tissues, very little is known about what effect this bacterium and its virulence factors exert on the cells of the blood-brain interface especially in the pre-clinical stages.

The authors thus pose the question, could a persistent level of *P.gingivalis* virulence factors in the circulation, renewed daily by chewing or tooth brushing [16] be sufficient to cause damage to the BBB in an otherwise healthy state?

The aim of this study was to investigate how the *P.gingivalis* virulence factors LPS and OMVs affected primary human cells in an *in vitro* BBB in the absence of the bacterial mother cell. This was assessed by investigating i) BBB integrity by transendothelial electrical resistance across the barrier, ii) how barrier permeability to fluorescent labelled LPS and dextrans was altered by the presence of *P.gingivalis* LPS and OMVs and iii) how LPS and OMVs interacted with the human brain microvascular endothelial cells.

METHODS

BBB MODEL

Primary-derived cell lines of human brain microvascular endothelial cells (HBMECs) (Neuromics USA) at passage 3, human brain vascular pericytes (HBVP) (ScienCell, USA) at passage 3 and human astrocytes (HA) cells (ScienCell, USA) at passage 3 were grown in flasks pre-coated with either AlphaBioCoat solution (Neuromics, USA) or Poly-L-Lysine 10 mg/ml (Sciencell, USA). Cells were cultured in complete endothelial cell growth basal medium (EBM) (Lonza, Switzerland), complete pericyte medium (PM) (Sciencell, USA) and astrocyte basal medium (ABM) (Lonza, Switzerland) with addition of human serum (Life Science Group, UK). The cells were grown to a confluency of 85-90% in humidified incubator at 37 ˚C, 5 % CO_2. The media was changed in all culture vessels every 48 hours until 50% confluent after this point every 24 hours. Trypsin (TrypLeexpress, Gibco, Thermofisher, USA) and

Hank's Balanced Salt Solution (Gibco, Thermosfisher, USA) were used for passaging cells. All observations of the cells were carried out under an inverted light microscope (Leica DMIL light microscope from Leica Microsystems GmbH, Germany). The viability and counting of the cells were assessed by using 1:1 Trypan Blue 0.4% (Sigma-Aldrich) and a haemocytometer [50,51]. Transwell™ multiple well plate with permeable polycarbonate membrane inserts (6.5 mm, 8.0 µm pore) (Corning, Fisher, UK) were coated with fibronectin (Sigma, UK) The HA and HBVP were seeded on the basolateral side of the insert and the HBMEC on the apical side [50]. The cells were maintained with medium of equal volume of PM, ABM and EBM (Lonza, Switzerland and Sciencell, USA) in a 37 °C humidified incubator under 5 % CO_2.

BBB INTEGRITY

After 4 days the integrity of the barrier model was tested by measuring the trans-endothelial electrical resistance (TEER) with an EVOM-2 instrument (WPI, UK). As the barrier becomes established the TEER value rise expressed in Ohm/cm^2 [52]. The triculture *in-vitro* BBB model was considered ready for testing when the TEER values reached an average of 260 Ohm/cm^2 [50,53]. The triculture barrier integrity were also assessed by application of FITC dextran 3 -5 kD, which was added to the apical compartment of the inserts and incubated for specific time periods according to the test protocols in the 37 °C humidified incubator under 5 % CO_2. At the specified time points in the test protocol samples were removed from the basolateral compartment and measured in a GENios Pro plate reader (Tecan, Austria) at 490 nm excitation and 520 nm emission (gain 40, 22˚C). Standard curves were produced from standard solutions of FITC 3-5 kDa and FITC-conjugated LPS in the range 0.04 to 100 µg/ ml.

CULTURE OF BACTERIA

P.gingivalis ATCC-BAA-1703 (strain FDC 381) was purchased from LGC limited (UK) in freeze dried vials. The bacteria were cultured according to the supplier's instructions. Briefly the *P.gingivalis* FDC 381 were cultured in ATCC medium 2722, supplemented tryptic soy broth (TSB) (TSB 3%, Yeast extract 0.5%, L-cystein hydrochloride 0.05%, Hemin (5 mcg/ml) with K_2HPO_4, Vitamin K1 (1mcg/ml) (Sigma Aldrich, UK)) on TSA with 5% sheep blood (Thermo Scientific, UK) and FAA agar with 7% horse blood Neomycin (75mg/l) (E and O, UK). All cultures were incubated at 37°C in an anaerobic chamber (Bactron, USA) using an anaerobic gas mixture of 5% H_2, 5% CO_2 and 90% N_2. The cultures were grown for 3 days. The optical density (OD) of the broth cultures were measured daily and selected for use when between OD_{655} 0.1 and 1 [54]. The cultures were Gram stained and imaged for quality control daily to ensure monoculture samples utilising a Gram staining kit (Merck, UK) and inverted light microscope using a X40 and X100 objective (Leica DMIL, Germany) and a Nicon DS-L4 camera and software.

ISOLATION OF OUTER MEMBRANE VESICLES OF P.GINGIVALIS

The outer membrane vesicles of *P.gingivalis* FDC 381 were isolated following the protocol used by Seyama et al. (2020)[54]. The bacterial culture in TSB was centrifuged at 2800 ×g for 15 min at 4 °C to separate the vesicles from the bacterial cells. The supernatant was passed through a 0.2 µm syringe filter (Millipore, UK) and then concentrated to under 1 mL by using an Ultra-15 Centrifugal Filter for the nominal molecular weight limit (NMWL) 100K (Sigma-Aldrich, UK). The concentrate was mixed with total exosome isolation reagent for culture (Life technologies, UK) and this was incubated at 4 °C overnight. The samples were centrifuged at 10,000 ×g for 60 min at 4 °C. The vesicles were eluted in 100 µL X1PBS. The TSB without bacteria was treated by the same method as a negative control. The diameter of the

outer membrane vesicles was measured and mono-dispersity ensured using a Zetasizer (Malvern Zetasizer Nano, Panalytical Instalment Ltd., UK) (55) and the concentrations of the samples was measured on the NanoDrop Spectrophotometer (280 nm) (Nanodrop 2000, Thermo Scientific, UK).

BBB RESPONSE TO P.GINGIVALIS VIRULENCE FACTORS

The *in vitro* BBB model response to virulence factors of *P.gingivalis* was tested by incubations with various concentrations (0.1 µg/ml, 0.3 µg/ml, 1 µg/ml, 10 µg/ml, 50 µg/ml and 100 µg/ml) of *P.gingivalis* LPS (Invivogen, France) and *P.gingivalis* outer membrane vesicles (OMV) and 1 µg/ml, 10 µg/ml, 50 µg/ml and 100 µg/ml of *P.gingivalis* LPS-FITC conjugate (Nanocs, USA). An experiment was also conducted with application of *P.gingivalis* LPS-FITC conjugate (Nanocs, USA) in combination with OMVs at 10 µg/ml. Control wells included no treatment (cell and media alone) and a cell blank (fibronectin insert, no cells). All measurements were made from each well in five times (TEER) or three times (Permeability, Papp), each plate had three wells (intraassay variability check). The test samples were diluted in complete medium of equal measures of EBM, PM and ABM. The test samples were placed in the apical compartment of the transwell and the TEER was measured at set time points (0.5,1, 2, 4, 24, 48 and 72 hours). At each time point the TEER values of the wells were measured 5 times and triplicate samples were collected from the basolateral compartment.

APPARENT PERMEABILITY OF THE BLOOD BRAIN BARRIER TO P.GINGIVALIS VIRULENCE FACTORS

Samples from the basolateral side of the BBB model were measured in the GENios Pro plate reader (Tecan, Austria) at 490 nm excitation and 520 nm emission (gain 40,

22˚C)[52], to quantify the appearance of fluorescent labelled LPS or FITC-dextran. The appearance from the apical to the basolateral compartment was calculated from standard curves of known concentrations of both FITC- dextran (3-5 kDa)(Sigma-Aldrich, UK) and the *P.gingivalis* LPS-FITC conjugate (Nanocs, USA) and the data from the standard curves were used to calculate the permeability (Papp) values in each experiment as shown in Equation 1.

$$P_{app} = \left(\frac{V}{A \times C_0}\right) \times \left(\frac{dQ}{dt}\right) \quad \textit{Equation 1}$$

where:

V = Volume of basolateral compartment (V= 0.6 cm^3)

A = surface area of the polycarbonate membrane (0.3 cm^2)

C_0= Initial concentration of the *P.gingivalis* LPS-FITC conjugate or FITC-Dextran in the apical well

dQ = concentration of *P.gingivalis* LPS-FITC conjugate or FITC-Dextran collected from the basolateral part (µg/ ml) (passing across the cell layer to basolateral side).

dt = Change in time (sec)

HUMAN IL6 ELISA

As a quality assurance measure to check all virulence factors (LPS, LPS-FITC conjugate and OMVs) were capable of producing an inflammatory response, all test reagents were evaluated for inflammasome activity by incubation (100 µg/ml) with HBVP for 4 hours in triplicate and the spent cell culture media was assayed for

human IL-6 release using a commercially available enzyme-linked immunosorbent assay (ELISA) kit (Sigma-Aldrich, USA). Test samples (spent media), controls (sample diluent buffer) and human IL-6 standards (100 µL) were added to the precoated 96 well ELISA plate. This was incubated at 4 ˚C for 24 hours with gentle shaking. After removal of the samples the wells washed with X1 wash buffer four times. Biotinylated detection antibody was added and incubated for 1 hour at room temperature with gentle shaking. The wells were washed four times with X1 wash buffer and HRP- streptavidin solution was incubated for 45 minutes at room temperature with gentle shaking. After washing four times with X1 wash buffer, ELISA colorimetric TMB reagent was added. This was incubated for 30 minutes at room temperature covered to exclude light while gently shaking. Then stop solution was added and the absorbance was measured in the 96-well plate immediately at 450 nm (Tecan, Austria). A standard curve was produced, the concentration of IL-6 in the samples was calculated.

IMMUNOFLUORESCENT IMAGING OF P.GINGIVALIS VIRULENCE FACTORS INTERACTIONS WITH TIGHT JUNCTION PROTEINS OF HBMEC CELLS

HBMECs (Neuromics, USA) were seeded at a density of 250000 cells/ml in black, tissue culture treated 24-well µ-plates (IBIDI at Thistle scientific, UK) and grown in EBM (Lonza, Switzerland) in a 37 °C humidified incubator under 5 % CO_2 for 8 days. The cells were tested for viability with Trypan Blue (Sigma-Aldrich, UK) and by visual daily inspection. On day 7 the cells were treated with 0.1 µg/ml and 0.3 µg/ml of unconjugated *P.gingivalis* LPS (Invivogen, France) or *P.gingivalis* outer membrane vesicles (OMV) diluted in EBM (Lonza, Switzerland) and incubated for 24 hours. After this incubation period the cells were fixed for IF protocol described below.

After incubation with the test samples the cells were washed in x1 PBS and fixed with 4% formaldehyde, washed and permeabilised with x1 PBS and 0.1% Triton-X (Sigma- Aldrich, UK) and blocked with 20 % normal goat serum (Stratech, UK) in 1x PBS with 0.1% Triton-X for 60 minutes. The cells were incubated with the primary antibody ZO-1 (D6L1E) Rabbit mAb (1:400) (Cell signalling, NL) at 4˚C for 12 hours and shaking and the secondary antibody Cy™5 AffiniPure Goat Anti-Rabbit IgG (1:800) (Jacsonimmuno, USA) for an hour at 4˚C. The cells were counter stained with DAPI(1:3500) (Stratech, UK) and imaged in a Zeiss Cell Observer system featuring the Zeiss definite focus, Colibri LED illumination and AxioVision 4 digital image processing software (Carl Zeiss Microscopy, Germany) detecting the signal for DAPI at ex:358 nm em:463 nm and Cy5 ex:646 nm em:664 nm. The images were viewed and processed using Zen 2.3 Lite software.

STATISTICAL ANALYSIS

The TEER and the permeability (Papp) data obtained from the *in vitro* BBB model was tested for homogeneity of variances and normality using the Shapiro-Wilk test. Difference between treatment groups was analysed using an ANOVA with Dunnett's post-hoc analysis or an independent t-test for comparison between independent experiments. The analysis was performed using the Statistical Package SPSS Version 26 and 27 (IBM, USA). Statistical significance was defined when (*) $P < 0.05$, and highly significant when (**) $P < 0.01$ and (***) $P < 0.001$.

RESULTS

BASELINE VARIABILITY AND MODELLING TEER CHANGES IN THE BBB MODEL

The baseline of the experimental model and optimisation was carried out to establish whether the primary cells and the 3-layer model were suitable for the planned experiments and not affected by the presence of the tracer compound. Prior to the start of the experiment, TEER values were consistent from day 7, with a typical variation of ± 10 Ω/ cm^2 over a 4 hour time period. Upon addition of either unconjugated *P.gingivalis* LPS (test wells), media (blank wells) or FITC (control wells) to the apical side of the BBB, there was a small initial dip in TEER at the start of the experiment that was attributable to movement artefact and slight disturbance of the BBB in all wells, typically this was ± 25 Ω/ cm^2 and recovery to baseline was observed in the control wells within 2 hours. The response of TEER in test wells upon addition of unconjugated LPS often showed a lower drop in TEER and that did not always recover to pre-baseline TEER. To determine whether the change in TEER was significantly different from baseline variation or movement artefacts, the pattern of response was modelled and the magnitude (ΔTEER), recovery time and rate of change were defined as shown in Figure 1 and were then used for statistical comparison between the control and test wells at different LPS concentrations.

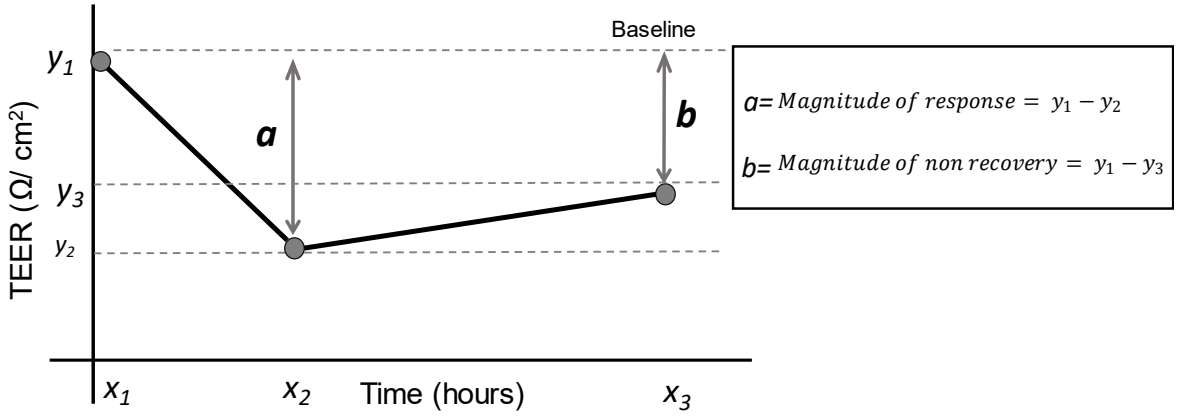

Figure 1. Modelling the magnitude and rate of change in TEER after application of

test sample to the in vitro BBB model

CONFIRMATION OF INFLAMMATORY RESPONSE OF VIRULENCE FACTORS TESTED, MEASURED BY HUMAN IL6 ELISA

In order to show that the virulence factors applied to the BBB model (unconjugated *P.gingivalis* LPS, FITC *P.gingivalis* LPS and *P.gingivalis* OMVs) had a biological response all samples were tested for induction of IL6 in HBPC prior to use. The inflammatory response of HBPC cells following exposure to unconjugated *P.gingivalis* LPS, FITC *P.gingivalis* LPS conjugated and *P.gingivalis* OMVs (all 100 µg/ml) after 4 hours of co-incubation, negative controls were media only. A standard curve was prepared and used to determine the concentrations of IL6 secreted by the cells in the test wells. This test was repeated every time a new conjugate reagent was used for the first time in triplicates. The results showed an elevated level of IL6 in the test samples compared to controls (data not shown). These results were seen as a positive control of the virulence activity in the samples tested.

EFFECT OF UNCONJUGATED P.GINGIVALIS LPS ON THE BBB INTEGRITY

The *in vitro* model was tested with un conjugated *P.gingivalis* LPS to assess the barrier response to this virulence factor. Application of unconjugated *P.gingivalis*. LPS to the BBB caused a significant decrease in TEER for 0.3 µg/ml ($P \leq 0.05$), 10 µg/ml ($P \leq 0.05$) and 100 µg/ml ($P \leq 0.05$) when compared the magnitude of change to the control well, where FITC alone or media alone were administered (Figure 2A). The magnitude of recovery of TEER values determined as the maximum TEER measured during the recovery phase. For all wells treated with unconjugated

P.gingivalis LPS there was still a deficit in recovery of the BBB integrity compared to the pre-incubation phase, as indicated by the deficit in TEER 72 hours post incubation relative to the baseline at time zero. The magnitude of deficit in TEER was significantly greater in the test wells where unconjugated *P.gingivalis* LPS was applied at 0.3 µg/ml ($P \leq 0.05$), 10 µg/ml ($P \leq 0.05$) and highly significant with 100 µg/ml ($P \leq 0.01$) compared to the control wells where FITC-alone was applied to the BBB (Figure 2B).

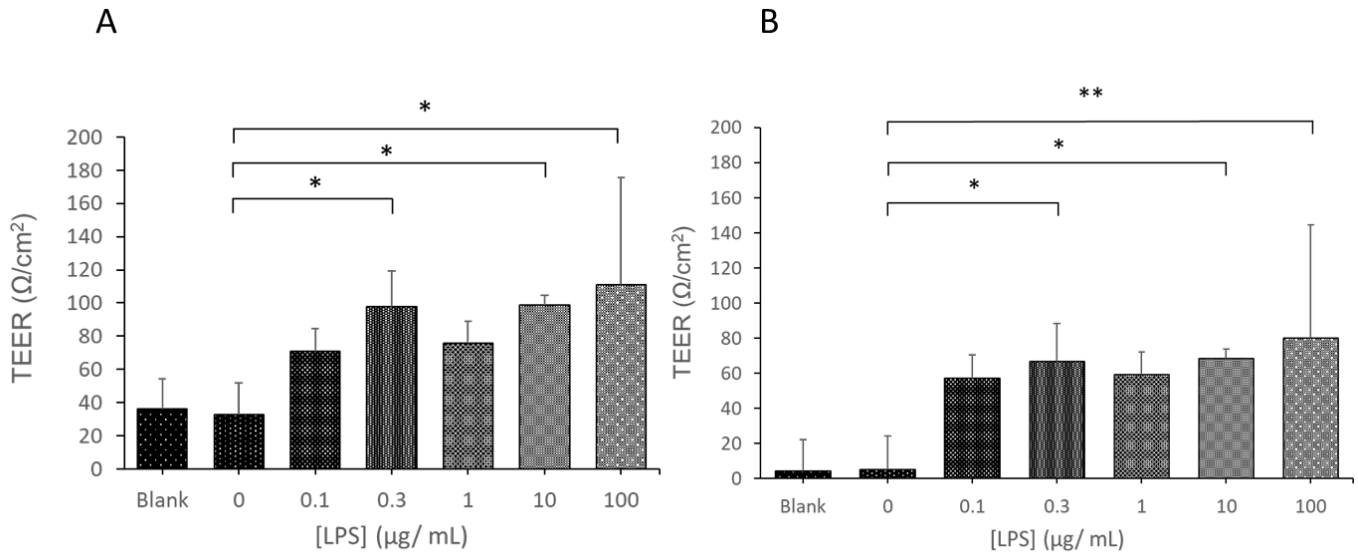

*Figure 2 Changes in BBB integrity measured by calculating the magnitude of decrease in TEER in response to application of unconjugated P.gingivalis LPS (A) and the magnitude of deficit in recovery of TEER 72 hours post application of unconjugated P.gingivalis LPS relative to initial baseline TEER (B).Statistical significance of response was measured using an ANOVA with Dunnett's post-hoc relative to the control (administration of FITC alone) where *P<0.05 and **P <0.01. Data represents mean ± SD from three wells and two experimental repeats (n=6).*

The integrity of the *in vitro* BBB model was also assessed by testing the wells with FITC-Dextran 3-5 kD as a marker of tight junction permeability. After incubation with unconjugated *P.gingivalis.* LPS or media (blank) for set time points. FITC-Dextran 3-5 kD was added to the wells and the fluorescent appearance of FITC-dextran on the basolateral side of the BBB was measured. It was observed that the FITC-Dextran

appeared earlier in the wells with 10 and 100 µg/ml of unconjugated *P.gingivalis* LPS following pre-incubation however this was not statistically significant relative to the blank wells and no significant concentration dependent effect in *P.gingivalis* LPS treatment related to FITC-dextran appearance was observed for the complete test period. The percentage appearance of FITC-dextran appeared to increase following longer exposure (24-72 hours) to *P.gingivalis LPS*, as shown in Figure 3C-E.

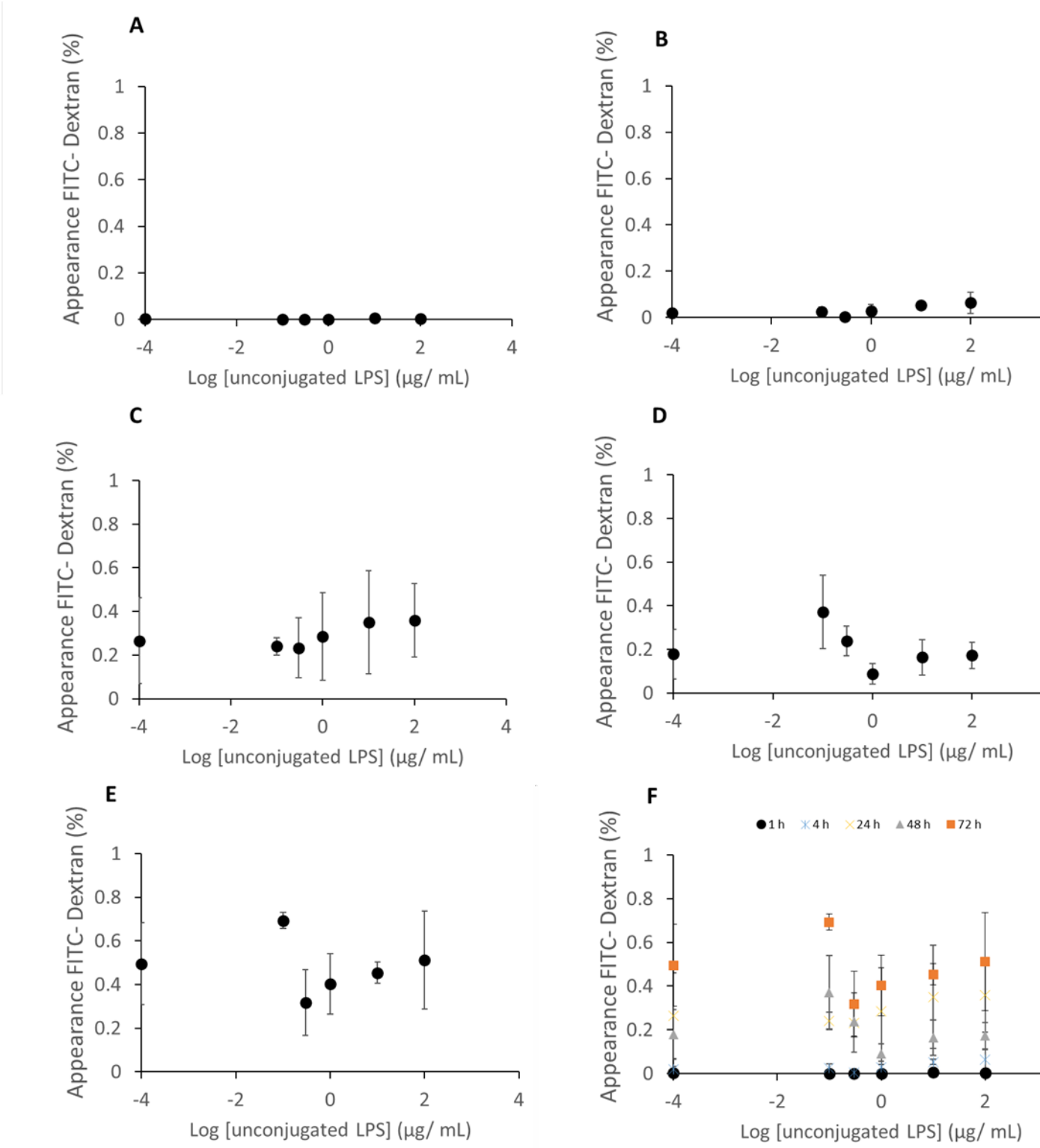

Figure 3. Shows the percentage of FITC-dextran (3-5 kDa) permeating through the in vitro BBB after incubation with increasing concentrations of unconjugated P.g. LPS (0-100 µg/ mL) for 1 h (A); 4 h (B); 24 h (C); 48 h (D); 72 h (E) and all exposure times compared together (F). Each data point represents mean ± SD from three wells and two experimental repeats (n=6).

The apparent permeability (Papp) of FITC-dextran (100 µg/ mL) after incubation for 30 minutes was calculated for three time points (60, 120 and 240 minutes) as described previously. Final Papp values at 60 min, 120 min and 240 min were found to be 1.04×10^{-8} +/- 2.3×10^{-8} cm/s, 8.7×10^{-8} +/- 1.7×10^{-7} cm/s and 4.8×10^{-8} +/- 4.7×10^{-8} cm/s.

EFFECT OF FITC-CONJUGATED P.GINGIVALIS LPS ON THE BBB INTEGRITY

To investigate potential transport across the *in vitro* BBB model a FITC labelled *P.gingivalis* LPS was applied to the established model and appearance of the conjugate was measured with the models integrity. It was shown that there were no significant differences in the magnitude of TEER response between the wells with application of all concentrations of FITC-*P.gingivalis* LPS conjugate and the control (FITC alone), however a decrease in TEER was observed in all wells after application of 1,10,50 and 100 µg/ml (Figure 4A). These wells did not appear to recover as well compared to controls (Figure 4B).

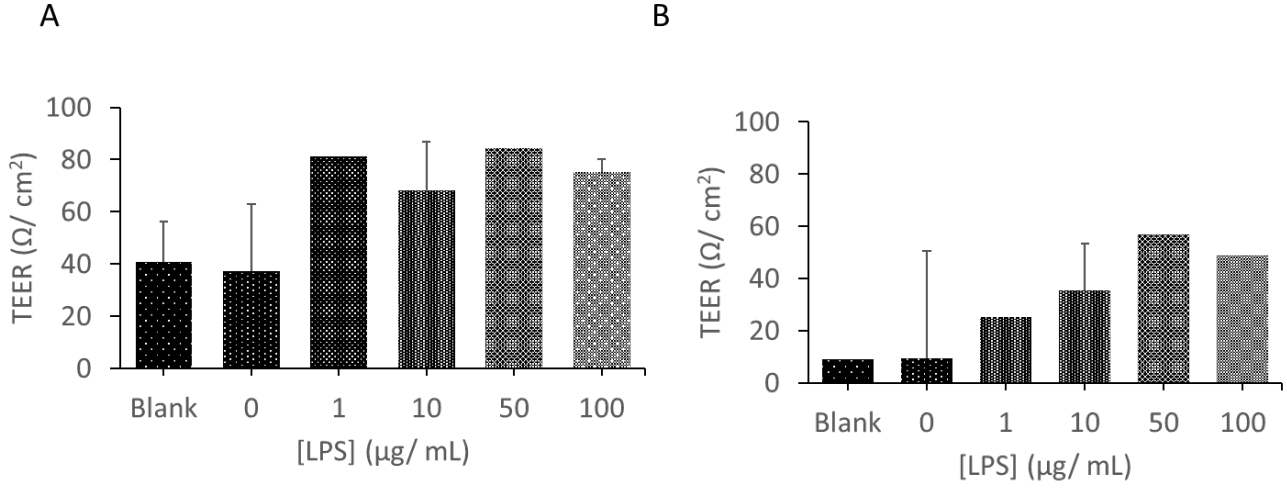

Figure 4 Changes in BBB integrity measured by calculating the magnitude of decrease in TEER in response to application of conjugated FITC-P.gingivalis LPS (A) and the magnitude of deficit in recovery of TEER 72 hours post application of conjugated FITC-P.gingivalis LPS relative to initial baseline TEER (B).No statistical significance of response was measured using an ANOVA with Dunnett's post-hoc relative to the

control (administration of FITC alone). Data represents mean ± SD from three wells and two experimental repeats (n=6).

The appearance of the FITC *P.gingivalis* LPS was greatest in the highest concentration (100µg/ml) at 1 and 4 hours (Figure 5A and 5B) and an increase of percentage appearance was observed with the concentrations 10 and 50 µg/ml as the experiment progressed at 24 and 48 hours (Figure 5C and 5D). The percentage appearance of the FITC *P.gingivalis* LPS in the basolateral compartment of the model did not exceed 5% during the duration of the experiments. A drop in the TEER values were seen to correlate with the appearance of the conjugate in all the wells of the higher concentrations (50 µg/ml and 100 µg/ml LPS) (data not shown).

All the wells were tested with FITC-Dextran at the end of each experiment to assess the final integrity of the barrier (data not shown).

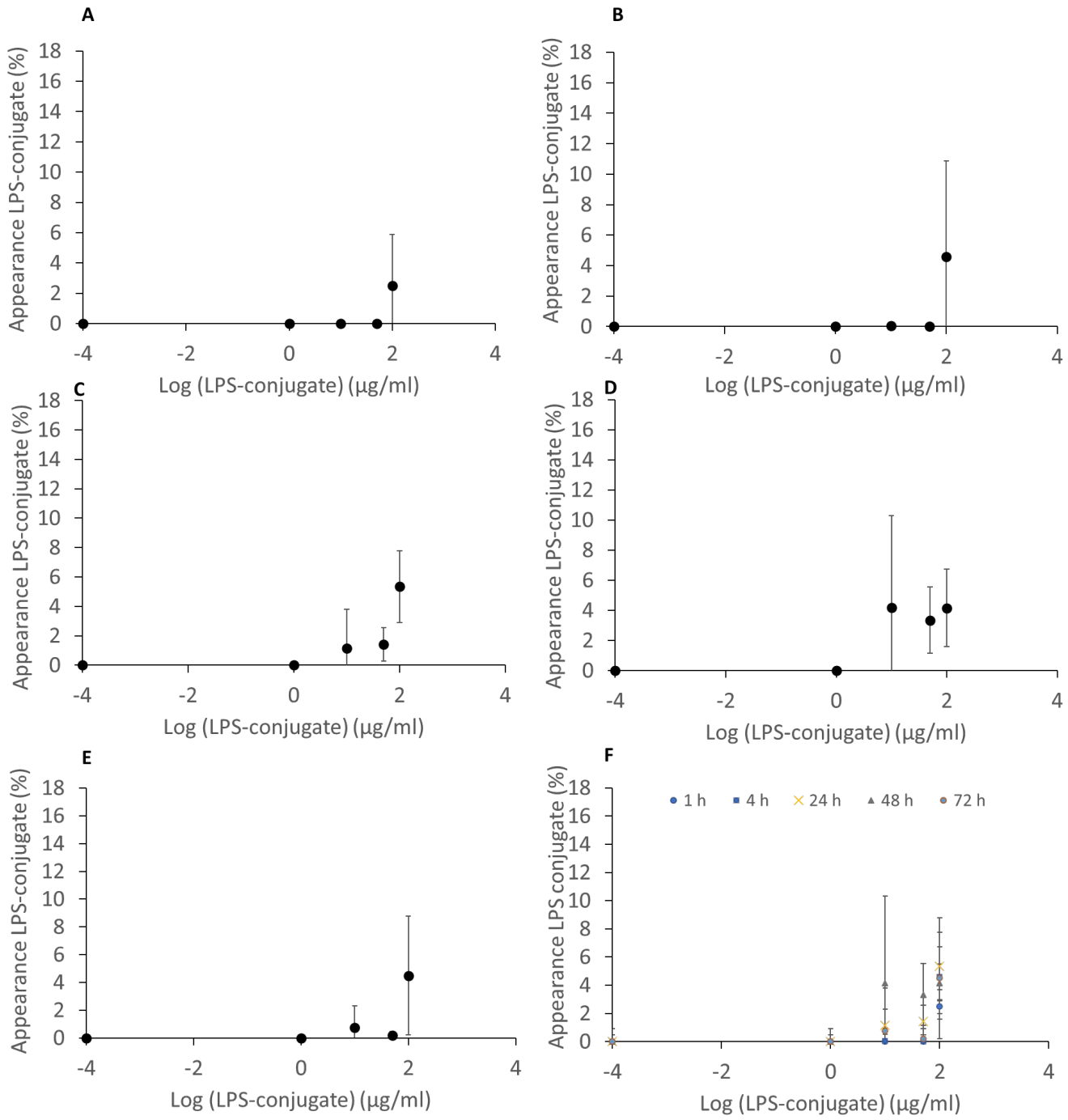

Figure 5 Percentage appearance of FITC *P.gingivalis* LPS conjugate on the apical side of the *in vitro* BBB model relative to the stock FITC *P.gingivalis* LPS administered to the basolateral side after 1 h (A); 4 h (B); 24 h (C); 48 h (D); 72 (E) and a comparison of all time points (E). *Statistical significance of response was measured using an ANOVA with Dunnett's post-hoc relative to the control (administration of FITC alone)*

*where *P<0.05 and **P <0.01. Data represents mean ± SD from three wells and two experimental repeats (n=6).*

EFFECT OF P.GINGIVALIS OMVS ON THE BBB INTEGRITY

The application of *P.gingivalis* OMVs showed similar patterns to the LPS study. The magnitude of decrease in TEER observed in response to treatment with OMVs was significantly different from the control group for the 0.1 µL/ mL (P<0.01); 0.3 µL/ mL (P<0.05); 50 µL/ mL (P<0.05) and 100 µL/ mL (P<0.01) (Figure 6A). This decrease in TEER did not recover to pre-treatment baseline for the wells treated with 50 and 100 µL/ mL *P.g* OMVs as the magnitude of deficit was highly significantly different to the control group (P<0.001), as shown in Figure 6B.

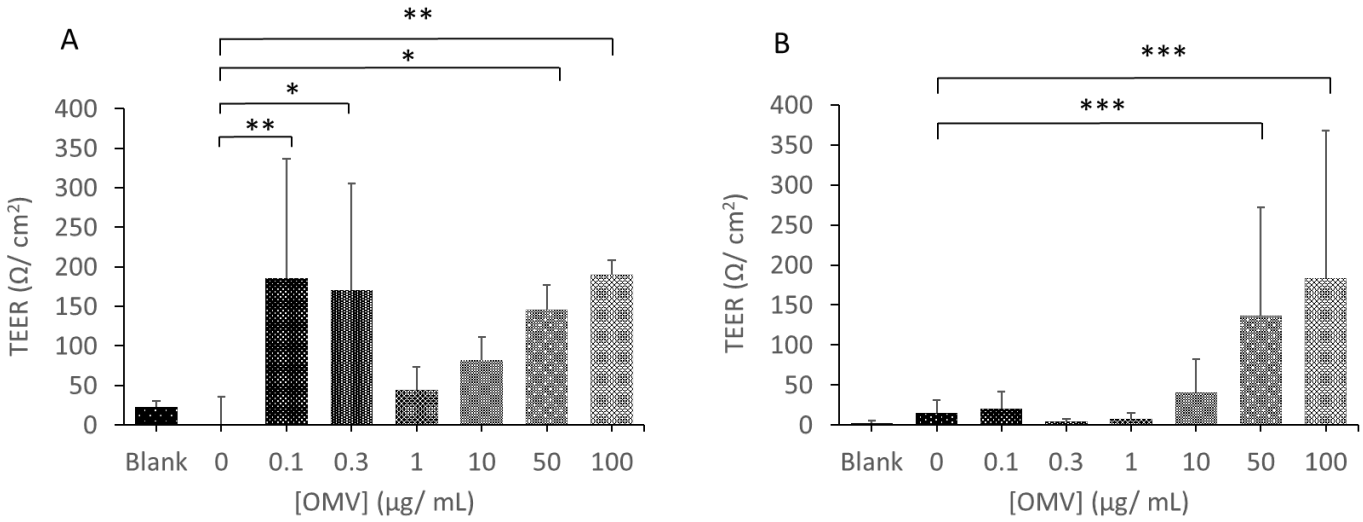

*Figure 6 Changes in BBB integrity measured by calculating the magnitude of decrease in TEER in response to application of P.gingivalis OMVs (A) and the magnitude of deficit in recovery of TEER 72 h post application of conjugated P.gingivalis OMVs relative to initial baseline TEER (B). Statistical significance of response was measured using an ANOVA with Dunnett's post-hoc relative to the control (administration of FITC alone) where *P<0.05, **P <0.01and and ***P <0.001. Data represents mean ± SD from three wells and two experimental repeats (n=6).*

Figure 7 shows the appearance of FITC-Dextran permeation following incubation of the *in vitro* BBB with increasing concentrations of *P.gingivalis.* OMV exposed for varying durations. Similar to the unconjugated LPS, the effect of OMV treatment on the extent of FITC-dextran permeation was fairly constant after the 12 hour exposure, but this time the permeation did appear to increase as the concentration of OMV increased (Figure 7C-E).

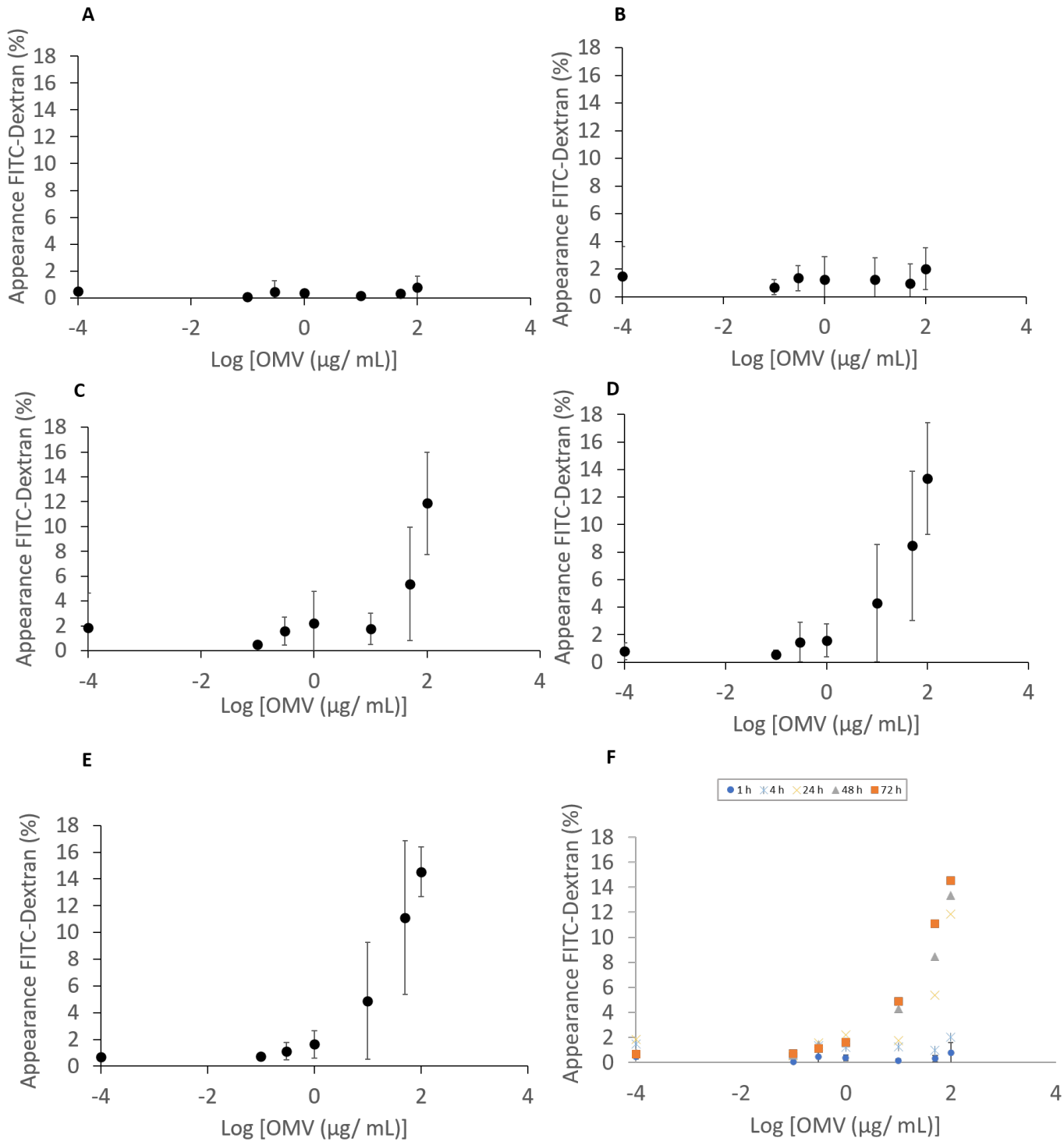

*Figure 7 Percentage appearance of FITC-dextran (3-5 kDa) on the apical side of the in vitro BBB model after application of P.gingivalis OMVs, percentage appearance relative to the stock FITC-dextran administered to the basolateral side after 1 h (A); 4 h (B); 24 h (C); 48 h (D); 72 (E) and a comparison of all time points (E). Statistical significance of response was measured using an ANOVA with Dunnett's post-hoc relative to the control (administration of FITC alone) where *P<0.05 and **P <0.01. Data represents mean ± SD from three wells and two experimental repeats (n=6).*

EFFECT OF P.GINGIVALIS OMV AND LPS ON THE BBB INTEGRITY

The *in vitro* BBB model was tested with FITC conjugated *P.gingivalis* LPS in the presence of a constant concentration of OMV to assess the effect the OMVs could potentially have on the appearance of the conjugated LPS in the basolateral compartment. The concentration of OMV was chosen (10 μg/ml) as this was the lowest which showed an effect in the BBB models integrity in the OMV only experiment previously (Figure 7D). The controls for the combined experiment were media only and OMV (10 μg/ml) only. The data was compared to the previous experiments with FITC *P.gingivalis* LPS only (Figure 5). The application of *P.gingivalis* LPS-FITC conjugate in conjunction with 10 μg/ml *P.gingivalis* OMVs showed a similar pattern in terms of response in the BBB model as seen in the previous experiments. The TEER responses in these experiments showed a significant difference in the 100μg/mL FITC *P.gingivalis* LPS conjugate with larger magnitudes of change in TEER compared to the controls ($P<0.05$) (Figure 8A). The higher the concentration of FITC *P.gingivalis* LPS with OMV, a reduced recovery was observed, although this was only significant in the highest concentration of 50 μg/mL and highly significant in the 100μg/mL FITC *P.gingivalis* LPS with 10 μg/ml OMVs (($P<0.05$ and ($P<0.001$)) (figure 8B). An increase in the permeability was seen especially after 24 hours where some of the increases were 5-fold compared to the experiment with *P.gingivalis* LPS-FITC conjugate application only, though this increase was not significant (Figures 5 and 9C).

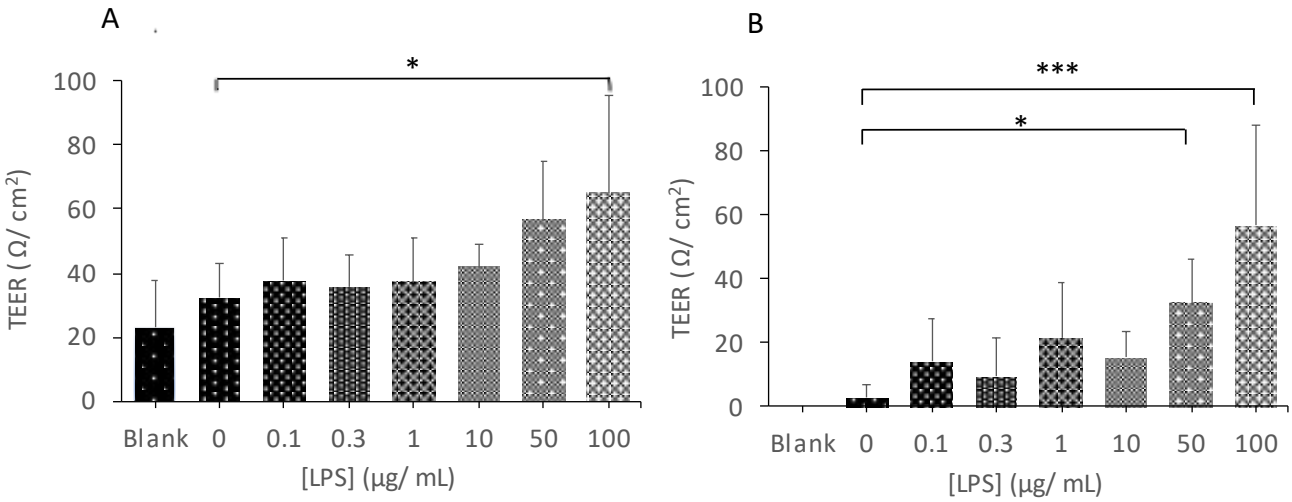

*Figure 8 Changes in BBB integrity measured by calculating the magnitude of decrease in TEER in response to application of FITC P.gingivalis LPS conjugate and 10 µg/ml P.gingivalis OMVs (A) and the magnitude of deficit in recovery of TEER 72 hours post application of of FITC P.gingivalis LPS conjugate and 10 µg/ml P.gingivalis OMVs relative to initial baseline TEER (B). Statistical significance of response was measured using an ANOVA with Dunnett's post-hoc relative to the control (administration of FITC alone) where *P<0.05 and ***P <0.001. Data represents mean ± SD from three wells and two experimental repeats (n=6).*

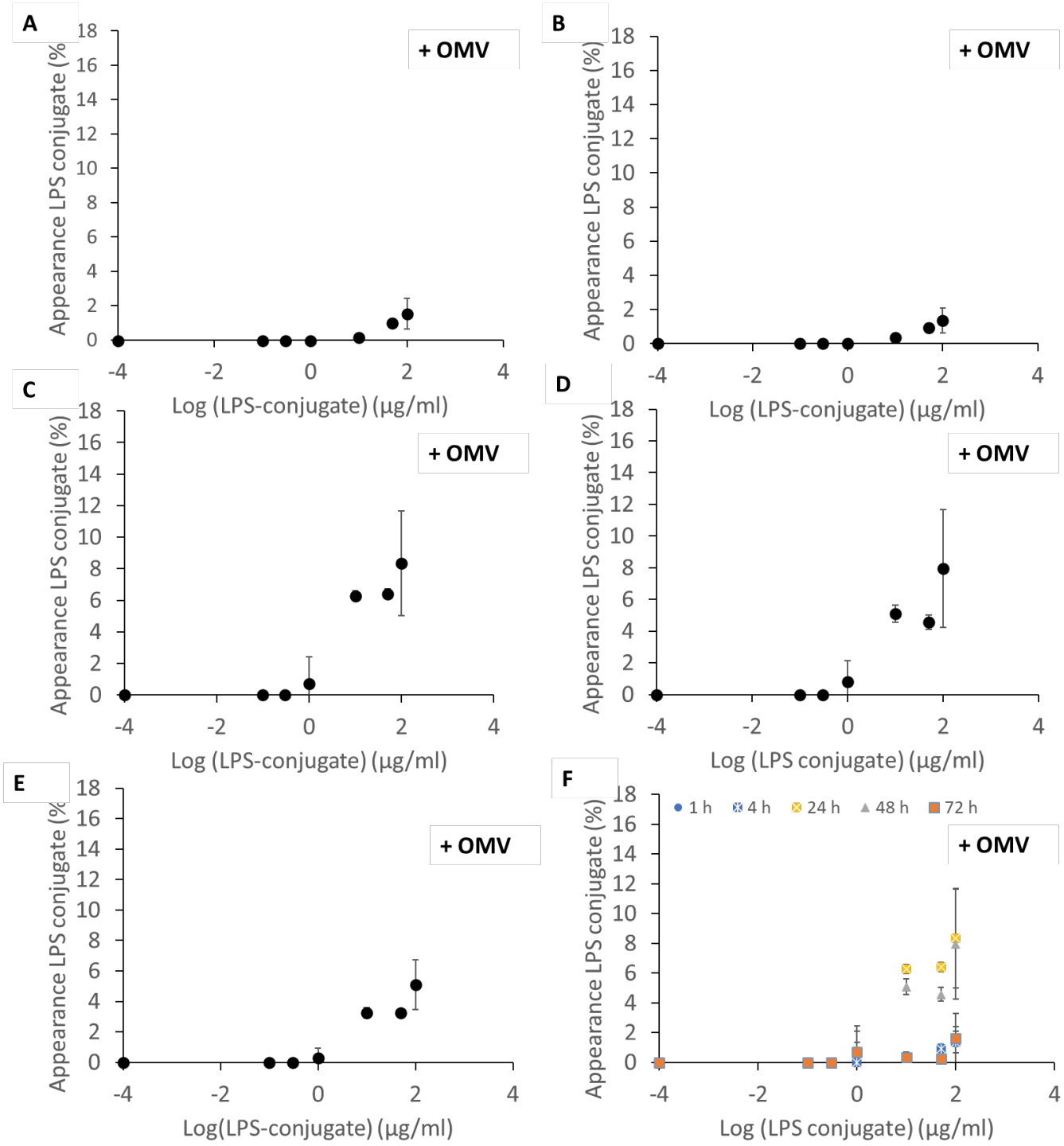

*Figure 9 Percentage appearance of FITC P.gingivalis LPS conjugate on the basolateral side of the in vitro BBB model relative to the stock administered to the apical side after 1 h (A); 4 h (B); 24 h (C); 48 h (D); 72 (E) and a comparison of all time points (E). Statistical significance of response was measured using an ANOVA with Dunnett's post-hoc relative to the control (administration of FITC alone) where *P<0.05 and **P <0.01. Data represents mean ± SD from three wells and two experimental repeats (n=6).*

ASSESSMENT OF VIRULENCE FACTORS INTERACTIONS WITH HBMEC MONOLAYERS MEASURED BY IMMUNOFLUORESCENCE MICROSCOPY

The experiments of application of virulence factors to the BBB model indicated a potential disruption of the barrier. These findings lead to the experiment with application of i) unconjugated *P.gingivalis* LPS (0.1 and 0.3 µg/ml) and ii) OMVs (0.1 and 0.3 µg/ml) to HBMEC cells in monolayer with an aim to determine how the observed BBB model disruption happened, all the experiments were repeated 3 times independently. The HBMEC cells were chosen for this experiment as these are the first cells coming into contact with the virulence factors in the *in vitro* model. The negative control cells (no virulence factors applied) showed the expected position of the ZO-1 protein at the cell-cell junctions and the signal of the ZO-1 protein appeared clear and well organised in these controls (Figure 10B and 10C). The concentrations for these experiments were based on observations after application of virulence factors of higher concentrations in the optimisation stages showed the HBMEC cells viability were consistently acceptable at these concentrations. All the test wells and controls were imaged using the same exposure times and all post exposure modifications were carried out to the same level with the Zen software. The HBMEC monolayer with application of *P.gingivalis* LPS showed no noticeable effect on the ZO-1 signal (Figure 10 D-F) (only 0.3 µg/ml shown) and similar observations were made in the wells with 0.1 µg/ml *P.gingivalis* OMV application (Figure 10 G-I) compared to the untreated controls (media only). The wells with application of 0.3 µg/ml *P.gingivalis* OMVs showed a more diffused signal from the ZO-1 proteins compared to untreated controls, which could appear as a reduction in the signal (Figure 10 J-L) though a change in the signal from the application of 0.3 µg/ml *P.gingivalis* OMVs were seen in all 3 repeat experiments it was not clear if the change was a displacement of the ZO-1 protein or reduced numbers as the

experiment here did not quantify the protein. All experiments were conducted with controls both for treatments, antibodies and counterstains and all showed the correct results.

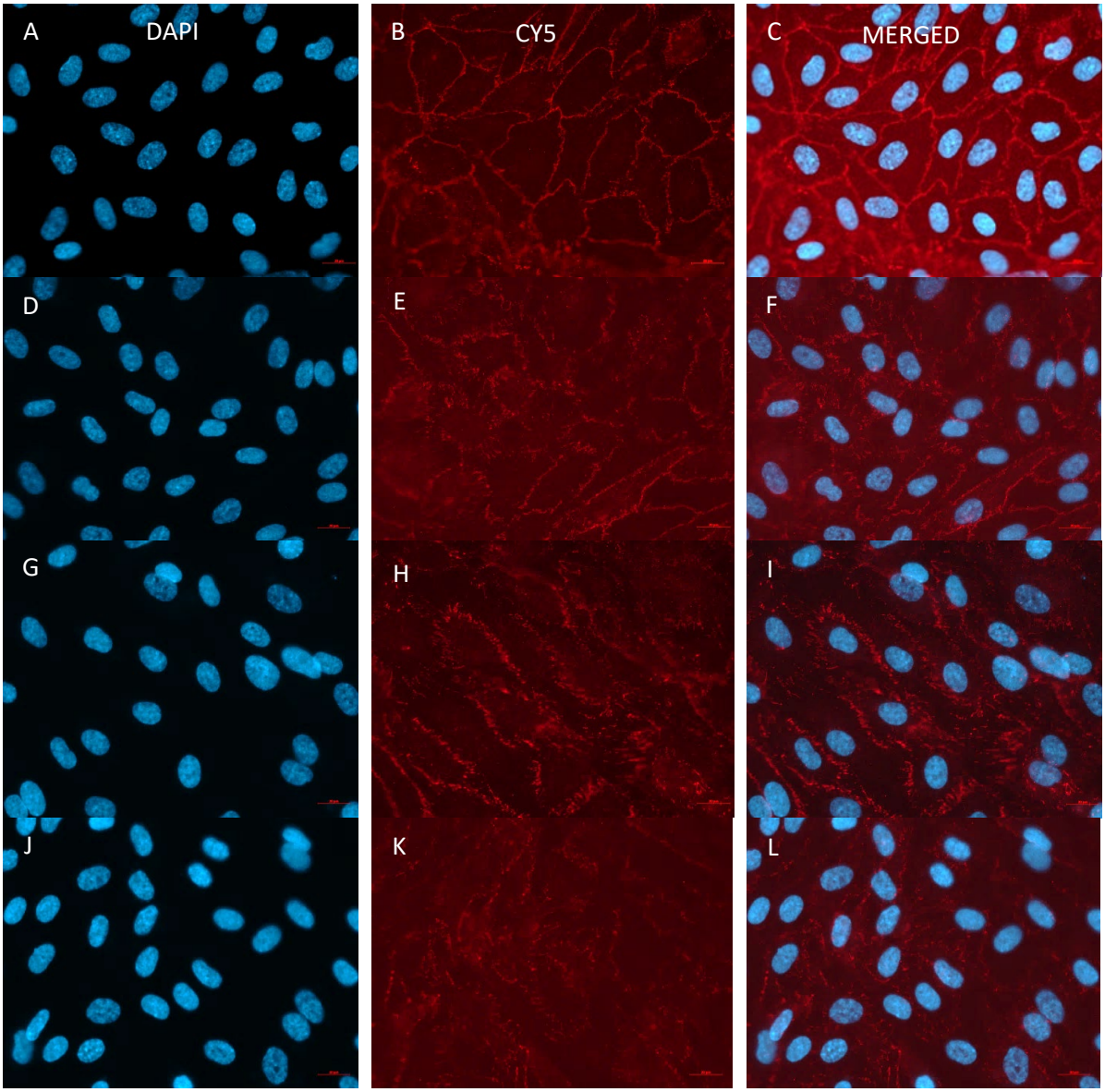

Figure 10. Immunofluorescent study of application of P.gingivalis virulence factors to HBMEC cells. HBMEC cells in monolayer were treated with EBM (A-C), 0.3 µg/ml P.gingivalis LPS (D-F), 0.1 µg/ml P.gingivalis OMVs (G-I) or 0.3 µg/ml P.gingivalis

OMVs (J-L) for 24 hours. Panels A, D, G and J show the nuclei stained with DAPI and detected at 358 nm (blue). Panels B, E, H and K show Cy5 signal detected at 646 nm (red) detecting the primary ZO-1 (D6L1E) Rabbit mAb. Panels C, F,I and L represent the composite pictures. Images were taken with 60x objective oil lens with the same exposure times. Scale bar 20 µm. (For interpretation of the reference to colour in this figure legend, the reader is referred to the article).

DISCUSSION

In this study we investigated the effect of *P.gingivalis* virulence factors on the cells in a human *in vitro* BBB model. Our observations regarding the movement of *P.gingivalis* LPS across to the CNS side of the model (Figure 5) and the enhancement of LPS appearance in the basolateral compartment in the presence of OMVs (Figure 9), supports findings from animal and other *in vitro* studies [17,19,20,27], though the methodology used in this study has not, to our knowledge been previously published. Designing robust human studies of chronic bacterial interaction at the BBB is challenging and making a link to sporadic AD must be carried out cautiously for numerous reasons, such as the latent period before AD pathological changes are first identified in brain tissues, and time to clinical symptomatology development both in the arena of multiple other risk factors associated with AD development. *In vitro* BBB models have been widely used for decades to investigate drug transport and individual disease processes, including Aβ clearance mechanisms in relation to AD [49,56]. Most BBB model studies investigating bacterial related interactions have focused on acute events [57,58].

The *in vitro* BBB model utilised in this study was developed by Kumar et al. (2014)[50] and subsequently validated for investigation of drug transportation across

651 the BBB . Although the main protocols for the model were established, some
652 adjustments had to be made for it to be meaningful in our investigation. It was vital
653 to establish continuous barrier integrity or function and to ensure the model was
654 suitable for the duration of testing and not affected by the application of FITC tracer
655 compounds. The concentrations of virulence factors applied were deduced from
656 previous studies [7,59] and by optimising the test protocols for which both high and
657 low doses were included. Starting with low concentrations, the virulence factors
658 assessment evidenced whether there was a concentration dependent relationship
659 with the endotoxin and OMVs which would indicate the resilience of the BBB model
660 to these virulence factors. After application of unconjugated *P.gingivalis* LPS, a clear
661 pattern emerged (Figure 1), of an initial drop in TEER values including the controls,
662 but it was observed that the drop in the wells which had endotoxin applied were
663 both greater in values and failed to recover as well as those in the control wells
664 indicating a lasting measurable effect in the BBB model barrier function. It was
665 concluded that the initial small drop in TEER values in the control wells (average of
666 25 ohms/cm^2) would need to be regarded as an artefact and test results within these
667 ranges were reviewed taking this into consideration by ensuring appropriate blank
668 (media only) and zero controls (FITC only) were included in every experiment where
669 appropriate. This artifact was not observed by Kumar et al. (2014) because the
670 protocols utilised here included continuously measuring of the TEER levels
671 throughout the experiments, whereas Kumar et al. used TEER as a quality control of
672 the barrier function before and after the experimental drug transport protocols.
673 This artifact can be explained as following the application of the Evom electrodes or
674 the media change, a short-lived disturbance could have occurred in the conductance
675 across the BBB model. This initial drop recovered in all the control wells and as the
676 protocol continued for 72 hours, a clear distinction between the test and control

wells was facilitated (data not shown).

A significant drop in TEER values was seen in wells tested with the concentrations of unconjugated *P.gingivalis* LPS (0.3, 10, 100µg/ml) (Figure 2A) and the recovery of TEER in these wells were also significantly less compared to controls (in 100 µg/ml highly significant, *P <0.01)* (Figure 2B). Furthermore, a significant drop in TEER was observed after application of *P.gingivalis* OMVs (0.3 and 50 µg/ml) (*P <0.05)* which were highly significant after application of 0.1 and 100µg/ml (*P <0.01)* (Figure 6A). The recovery in the wells with 50 and 100µg/ml had a highly significant (P *<0.001)* deficit compared to the controls (Figure 6B), indicating that these virulence factors affected the *in vitro* BBB model in a prolonged and negative fashion. However, at lower concentrations (0.1,0.3 and 1 µg/ml) some of the TEER value reductions were temporary followed by partial or complete recovery (Figure 6B). The authors suggest this may have arisen as a result of i) an initial apoptosis event subsequently overcome by the surviving neighbouring cells expanding to repair the damaged area or ii) an initial disruption of the tight junction complexes followed by a reparatory upregulation event. These observations are important as they indicate the cells of the BBB model have an ability to recover if the endotoxin is applied at a low level. Applied to a human clinical scenario this means that after a low level, low frequency endotoxin contact with the BBB, the NVU cells appear to retain the ability to preserve the barrier's integrity. Clinically this could correlate with the adoption of an improvement in oral hygiene or if systemic risk factors for PD, such as diabetes, were eliminated or reduced.

The wells demonstrating less ability to recover their TEER values, could indicate that the cells in those wells were unable to survive or expand, or the LPS and OMV could have influenced the continuity of the cell layer either by causing pyroptosis [38], apoptosis or irreversible tight junction disruption [43,60]. It was recorded that there

were reductions in TEER readings in the wells receiving FITC *P.gingivalis* LPS conjugate in media compared to controls and that these TEER levels also did not recover as well, though none of these TEER value differences were statistically significant compared to the controls (Figure 4A and 4B).

The appearance of FITC dextran in the basolateral compartment gave an indication of disruption to the barrier integrity after unconjugated *P.gingivalis* LPS and OMV application at various concentrations. Average Papp values were then calculated at 60 min, 120 min and 240 min and were found to be 1.04×10^{-8}cm/s, 8.7×10^{-8} cm/s and 4.8×10^{-8} cm/s. In permeability assays for drug transportation poor permeability is indicated by Papp values of 0 - 1.4×10^{-6} cm/s and high permeability by values in the range of 5×10^{-5} - 9×10^{-5} cm/s. The low calculated Papp values in our study suggest that the Papp for the tracer compound FITC-dextran were low indicating the BBB model retained its overall barrier function for the first two hours, though allowing enough permeation to measure a difference between test wells (Figure 3). The most significant effect in the models TEER measurements were observed in the wells with concentrations of unconjugated LPS and OMV at 0.3 µg/ml, 10 µg/ml, 50 µg/ml and 100 µg/ml and contextualised to a theoretical physiological condition, the lowest of these values, 0.3 µg/ mL is most clinically applicable [7,59].

The changes in the BBB model cells after application of the FITC-*P.gingivalis* LPS in conjunction with 10 µg/ml of *P.gingivalis* OMV showed a significant difference in the magnitude of change in the TEER values and a significant deficit in recovery of the values (highly significant in 100 µg/ml FITC-*P.gingivalis* LPS) which, highlighted the potency of the OMVs containing gingipains pr (Figure 8).

The TEER measurements of an *in vitro* BBB model reflect the ionic conduction paracellularly in the cell layers, whereas the percentage appearance of a tracer compound in the BLC represents paracellular waterflow associated with increased pore size at the tight junctions [52]. Transcellular ion transport function and paracellular permeability of solute transport are differentially regulated [52], where the factors affecting perfusion of a molecule across the BBB is size, shape and lipophilicity. TEER is a valuable assessment of the in vitro BBB integrity as it is easy to quantify and if carried out with care, non-invasive. It is however important to be aware of the limitations of TEER measurements, where variations can occur due to factors such as medium content, temperature and the passage numbers in the cell lines at the time of measurements [52]. As the protocols in this study were performed under the same conditions using the same equipment and cell passage numbers, some of the potential variables could be excluded. As an example, the EVOM probe was calibrated in the same manner before each measurement and five readings were taken from the individual wells with each experiment, providing the authors with confidence in the longitudinal magnitude of change and TEER endpoint results

The biphasic TEER pattern observed in all the virulence factor application protocols (data not shown) could potentially also be explained by the exponential growth of the cells in the wells or a cell response to the applied reagents such as an upregulation in the cells, making the TEER appear to recover with time. This would suggest that any disruptions to the BBB cells which could be measurable by TEER, would have to counteract this progression in cell density and tight junction maturation or would otherwise go undetected. It is most likely that the recovery of the BBB observed in the wells, throughout our experiments, reflects an increased number of cells in the BBB as there was no other significant increases in permeability

753 recorded for the remainder of the test period when further endotoxin was applied,
754 or the concentrations of LPS added were not high enough to induce measurable
755 changes to the percentage appearance in the BLC (Figures 3 and 5).

756 Previous validation studies of *in vitro* BBB models like ours have shown that a TEER
757 (read) value in the range of 120 – 130 ohms/cm^2 is enough for transport studies [61].
758 When setting up the BBB model for testing transport and permeability in this project
759 the aim was to achieve values of TEER (read) – TEER (blank) ≥ 260 ohms/cm^2 [61],
760 this was achieved in all the
761 protocols.

762 A tracer compound used in an *in-vitro* BBB model can potentially interfere with the
763 test reagents and affect the integrity of the barrier [52]. This issue was addressed by
764 using test wells with FITC-dextran only throughout the study. Fluorophore and dye
765 tracer compounds are not always sensitive enough to show subtle changes in barrier
766 model permeability [52] which is a weakness of this type of study and bias can be
767 introduced if the sensitivity in the measuring equipment is not high enough to pick
768 up the compound at small levels. The FITC dextran molecule used here has been
769 shown to cross the BBB model via intercellular diffusion [62] and any increase in
770 intercellular channels would allow greater amounts to pass into the BLC. This study
771 demonstrated that the appearance of FITC dextran into the BLC occurred early
772 (between 1 and 4 hours) after the initial application of unconjugated *P.gingivalis* LPS,
773 particularly with the testing of the higher concentrations of LPS, but subsequent
774 applications failed to demonstrate any clear correlation between the concentration
775 of applied endotoxin and the percentage appearance measured in the BLC. This
776 implies that the higher concentrations of LPS were able to induce an increase in
777 paracellular flow, possibly by increasing paracellular gaps, at initial application

compared to controls (Figure 3). However, further increases were not demonstrated by additional applications implying a finite capacity for paracellular flow increase. These findings were supported by the Papp calculations of the FITC dextran throughout the protocols and the percentage appearance values which also remained low after application of unconjugated LPS. The levels of FITC-dextran appearance seen throughout the unconjugated LPS experiments were persistently low with the maximum appearance at 0.7% (Figure 3) which is encouraging in terms of demonstrating the quality of the barrier model [50]. In comparison the percentage appearance of FITC dextran seen in the OMV alone experiment were higher with the maximum percentage appearance being 15-fold higher than the LPS alone (Figure 7). The maximum percentage appearance of the FITC LPS conjugate in the BLC was 5% during the experiments (Figure 5) and a small increase to 8% maximum percentage appearance was observed when 10 µg/ml was added to the FITC-LPS conjugate (Figure 9). The increased percentage appearance in the OMV alone (Figure 7) could be explained by the presence of the proteolytic enzymes or gingipains within the OMVs which could also explain the increased permeability of the FITC *P.gingivalis* LPS in the presence of 10 µg/ml of OMV (Figure 9). The enzymes could create greater gaps between the barriers cell layers allowing greater perfusion of the molecules to the BLC. The differences in percentage appearance between the FITC *P.gingivalis* LPS and the FITC dextran molecules (Figures 3 and 5), where the percentage detected in the BLC of FITC P.gingivalis LPS was approximately 5 fold larger than FITC dextran appearance after unconjugated LPS, can be explained as a potential difference in the virulence between the two compounds (conjugated and unconjugated LPS) inflicting different effects on the pore sizes within the barrier, or variances in the size, shape and/or lipophilicity between FITC dextran and FITC LPS molecules could attribute to this observation. The *P.gingivalis* LPS could also affect

804 the cells of the BBB model differently at receptor level after being conjugated , even
805 though the LPS product used for both reagents originated from the same source.

806 The immune response of the *P.gingivalis* LPS, *P.gingivalis* LPS FITC conjugate and
807 *P.gingivalis* OMV utilised in the experiments was examined by an IL-6 ELISA after
808 application for 4 hours to HBPC. IL6 is a proinflammatory cytokine and the induction
809 of this cytokine would give an indication of the biological activity of the virulence
810 factors utilised in this study, as the presence of LPS would induce TNF-α pathways in
811 the HBPC to release IL6 [63]. The response and induction of IL-6 from all reagents
812 measured in the cell media, were of a similar quantity and levels were increased
813 compared to controls (media only)(data not shown).
814 The unconjugated *P.gingivalis* LPS used in this study was the standard preparation
815 (defined by preparation by supplier) which has been noted to induce a stronger
816 inflammatory response than the pure version (both supplied by Invivogen) possibly
817 as a result of impurities of lipoproteins in the standard preparation, activating TLR2
818 as well as TLR4 [64]. Furthermore, the standard *P.gingivalis* LPS has also been found
819 to show a stronger inflammatory response in human periodontal stem cells after 24
820 hours than the pure version (64). In our BBB protocols we saw an increased response
821 at 24 hours with both *P.gingivalis* LPS and OMVs which indicates that the induced
822 response could be more complex than a simple apoptosis of the cells and involve
823 inflammatory pathways affecting the integrity of the barrier. The OMVs applied in
824 this study were extracted from a culture of the laboratory strain *P.gingivalis* FDC 381
825 which is classed as a less virulent *P.gingivalis* strain but has a high ability to be
826 internalized in human cells [65]. This non-capsular strain has been shown to be a
827 strong immune stimulant, (even activating TLR2) a property attributed to an intact
828 fimB allele but with a less gingipain activity [66]. It is possible that the difference in
829 appearance of the *P.gingivalis* LPS FITC conjugate on the CNS side of the model with

and without the presence of the OMVs would have been more significant if a less virulent *P.gingivalis* LPS product had been used such as the purified product mentioned previously.

The *in vitro* BBB model has limitations such as the delicate nature of working with primary-derived cell lines and the measurements derived from this study do not divulge much information about a cellular level activity. There is an increased consensus that to gain more accurate knowledge of AD, microbial pathology human models need to be developed, as pathological and inflammatory pathways in rodents significantly differ from humans [6, 31] especially in relation to molecules such as LPS [38]. The expression in the author's human BBB model cells is closer to the *in vivo* state than a murine model and there is potential in our model to gain further cellular level information. The role of microglial cells in neurodegeneration is undisputed and expansion of this model to include human microglial cells could broaden the applications for this type of protocol. In addition, also BBB organoids could potentially be applied to this type of study [67].

There is evidence to suggest that *P.gingivalis* may not need to enter the brain to cause neuroinflammation [38]. Even healthy humans have been shown to have low levels of LPS in their blood [68], but this is found to be elevated in AD and PD patients [69,70,71]. AD patients have been found to have 2-3 times as much LPS in the brains as healthy individuals [72]. LPS is released from the bacteria either when it is degraded or when outer membrane vesicles are released [38] and the GI microbiome has been shown to be the main contributor to systemic presence. LPS has been suggested as an intermediary between bacteria and the CNS at low levels (physiological) conditions [73] in rodents, and a lipo-protein transport mechanism to the CNS has been suggested, but it is not yet known exactly how LPS enters the brain

in humans. It is possible that transport mechanisms are responsible for the appearance of the LPS on the BLC (CNS) side of the model used in this study and this topic warrants further investigation, OMVs are known to have the ability to be internalised by human cells which is another avenue to explore.

This study however has demonstrated that the integrity of a BBB model is reduced by the presence of *P.gingivalis* virulence factors seen by a measurable reduction in TEER levels and making the barrier more permeable and the subsequent increased appearance of LPS in the BLC (CNS side of BBB).

Bacterial LPS has been found to change the permeability of the BBB at high doses [74] as seen in sepsis causing significant CNS disability. *P.gingivalis* LPS has the potential to cause neuroinflammation via the blood directly acting at the BBB, by inducing pro-inflammatory cytokines, initiating pro inflammatory pathways in the tissues of the neuro vascular unit and activating microglial cells without entering the brain [38]. In addition, this study has indicated that *P.gingivalis* LPS also has the potential to cross the BBB as seen in the FITC *P.gingivalis* LPS experiments, potentially explaining how systemic circulating LPS could induce neuroinflammation. The subsequent immunological response to LPS is well documented (for a review see 44) and the toxicity of an endotoxin is determined by how the host reacts to it [75]. Both immunological activation and tolerance [76,77] can explain how chronic exposure to even medium and low levels of *P.gingivalis* LPS could lead to neurodegeneration by induction of pro-inflammatory pathways and activation of microglia and it is plausible that a low concentration of *P.gingivalis* virulence factors can induce damage to the NVU cells [78,79]. Here we have shown, in a BBB model, that whole bacteria do not need to be present as *P.gingivalis* LPS and OMVs have the armoury to induce alteration of the barrier integrity providing access to the CNS tissues. A question remains about how much damage, over what period of time is

881 required, before the balance is tipped towards a path where the BBB cells cannot
882 recover?

883 The aim of applying *P.gingivalis* LPS and OMVs to a HBMEC monolayer was to
884 investigate whether the changes observed in the BBB model protocols could be seen
885 at a cellular level and to determine how these changes occurred. The negative
886 control cells (no virulence factors applied) showed the expected position of the ZO-1
887 protein at the cell-cell junctions [80] with the signal of the ZO-1 protein appearing
888 well organised (Figure 10B and 10C). The HBMEC monolayer with application of
889 *P.gingivalis* LPS showed no noticeable effect on the ZO-1 signal (Figure 10 D-F) (only
890 0.3 μg/ml shown) and similar observations were made in the wells with 0.1 μg/ml
891 *P.gingivalis* OMV application (Figure 10 G-I) compared to the untreated controls
892 (media only). The wells with application of 0.3 μg/ml *P.gingivalis* OMVs showed a
893 more diffused signal from the ZO-1 proteins compared to untreated controls, which
894 could appear as a reduction in the signal (Figure 10 J-L). All the test wells and
895 controls were imaged using the same exposure times and all post exposure
896 modifications were carried out to the same level with the Zen software. Though a
897 change in the Cy5 signal after the application of 0.3 μg/ml *P.gingivalis* OMVs were
898 seen in all 3 repeat experiments compared to untreated controls, it was not clear if
899 the change was a displacement of the ZO-1 protein or reduced numbers as the
900 experiment here did not quantify the protein. ZO-1 is a tight junction adaptor
901 protein connecting the actin skeleton to tight junctions such as claudin and the
902 binding of Zo-1 to actin is essential for regulation of permeability in epithelial cells
903 [81]. Tornavaca et al. (2015)[82] showed that in primary endothelial cells ZO-1 is a
904 central regulator of tight junctions depending on the strictly endothelial specific
905 adhesion molecule vascular endothelial (VE) -cadherin. These endothelial junctions
906 were found to influence the spatial actomyosin organization, cell–cell tension and

migration across the endothelium, but also angiogenesis and barrier formation. This study used human dermal microvascular endothelial cells (HDMEC-c) and not HBMECs, but this places ZO-1 central to the development, integrity and maintenance of the BBB and if *P.gingivalis* OMVs are able to disrupt the functionality of ZO-1 this could have devastating consequences to the integrity of the blood brain interface. ZO-1 is a large phosphoprotein and post-translational alterations such as phosphorylation would lead to ZO-1 dissociation from the tight junction complex [83], which could potentially be how *P.gingivalis* virulence factors affect this protein and explain the TEER and diffusion changes observed in our study, where notably the application of *P.gingivalis* OMVs had the greatest effect on both measurements.

Multiple studies have investigated the effect of *P.gingivalis* LPS and OMVs on cells, both human and animal, but not on cells of the human BBB. It was clear from our study that the *P.gingivalis* LPS both unconjugated and FITC conjugated and OMVs did affect the cells of this *in vitro* BBB model and caused barrier integrity changes. There is potential to investigate more nuanced changes in the cells by using the protocol described here and applying further protocols which could also potentially reveal changes at the lower concentration of LPS level which the TEER and percent appearance methods did not have the sensitivity to reveal.

CONCLUSION

The two virulence factors of *P.gingivalis* (LPS and OMVs) were seen to induce changes in the human *in vitro* BBB model cells. Unconjugated *P.gingivalis* LPS, FITC conjugated *P.gingivalis* LPS with 10 µg/ml of OMV and OMVs alone had a significant effect on the integrity of the *in vitro* BBB model which were measurable by TEER showing a significantly greater magnitude of change after application and a significant deficit in recovery of the models TEER values. These changes were also

observed after application of virulence factors at a physiological relevant level (0.3 µg/ml). The application of *P.gingivalis* OMVs resulted in the most significant magnitude of change in the TEER values of the barrier and the most significant deficit of recovery. These experiments also confirmed that endotoxin from *P.gingivalis* conjugated with FITC was able to cross the barrier model and that the percentage of LPS conjugate appearing on the CNS side of the model were increased by the presence of *P.gingivalis* OMVs. The ZO-1 proteins in a HBMEC monolayer model showed disruption after contact with *P.gingivalis* OMVs compared to controls.

Further investigations at cellular level are warranted to contribute to the knowledge pool of how endotoxin from periodontal disease could have an influence on neuroinflammatory states and potentially contribute to or exacerbate neurodegeneration. If these observations are applied to the human BBB, then infection with *P.gingivalis* and their inflammagens LPS and OMVs could cause damage to an otherwise healthy and non-predisposed individual. It is tempting to attribute the link between sporadic Alzheimer's Disease and periodontal disease to the effect of this multi-talented pathogen, when the chronicity of the inflammatory state seen in established periodontal disease could be the main culprit. This highlights not only the need for good oral hygiene, but also the importance of diagnosis and optimal management of dental patients presenting with unstable periodontal disease. Until there is a therapeutic remedy which can protect the BBB from chronic inflammation, prevention remains the key.

*ACKNOWLEDGEMENTS*AP acknowledges funding from the Faculty of Dental Surgery, Royal College of Surgeons England pump priming grant and the kind donation from The Norah and Fred Roberts Memorial Trust.

CONFLICT OF INTEREST

The authors declare no conflict of interest.

Supplementary information:

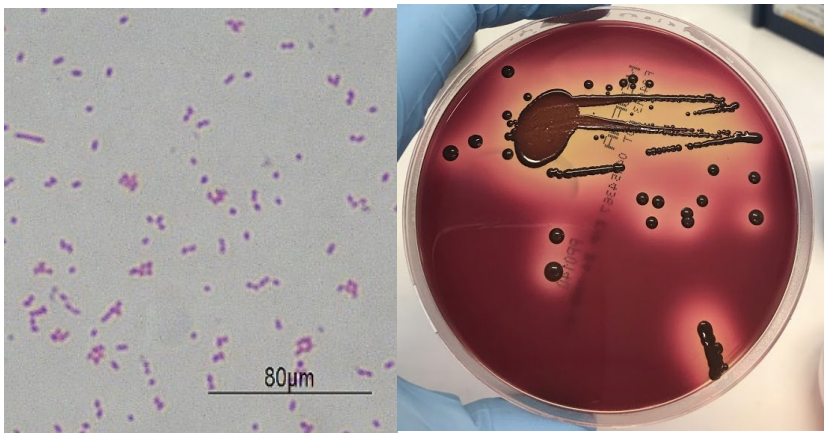

P.gingivalis FDC 381 Gram stain and on FAA Neomycin (E&O, UK) shows coccobacillus at x100 and Black stain colonies of the strain with haemolytic halos on NEOFAA agar.

References

1. Alonso R, Pisa D, Marina AI, Morato E, Rábano A, Carrasco L. Fungal infection in patients with Alzheimer's disease. J Alzheimers Dis. 2014;41(1):301-11. doi: 10.3233/JAD-132681. PMID: 24614898.

2. Miklossy J. Bacterial Amyloid and DNA are Important Constituents of Senile Plaques: Further Evidence of the Spirochetal and Biofilm Nature of Senile Plaques. J Alzheimers Dis. 2016 Jun 13;53(4):1459-73. doi: 10.3233/JAD-160451. PMID: 27314530; PMCID: PMC4981904.

3. Itzhaki RF, Lin WR, Shang D, Wilcock GK, Faragher B, Jamieson GA. Herpes simplex virus type 1 in brain and risk of Alzheimer's disease. Lancet. 1997 Jan 25;349(9047):241-4. doi: 10.1016/S0140-6736(96)10149-5. PMID: 9014911.

4. Pritchard AB, Crean S, Olsen I, Singhrao SK. Periodontitis, Microbiomes and their Role in Alzheimer's Disease. Front Aging Neurosci. 2017 Oct 24;9:336. doi: 10.3389/fnagi.2017.00336. PMID: 29114218; PMCID: PMC5660720.

5. Braak H, Braak E. Morphologie des Morbus Alzheimer [Morphology of Alzheimer disease]. Fortschr Med. 1990 Nov 20;108(33):621-4. German. Erratum in: Fortschr Med 1991 Mar 20;109(8):186. PMID: 2289729.

6. Fulop T, Tripathi S, Rodrigues S, Desroches M, Bunt T, Eiser A, Bernier F, Beauregard PB, Barron AE, Khalil A, Plotka A, Hirokawa K, Larbi A, Bocti C, Laurent B, Frost EH, Witkowski JM. Targeting Impaired Antimicrobial Immunity in the Brain for the Treatment of Alzheimer's Disease. Neuropsychiatr Dis Treat. 2021 May 4;17:1311-1339. doi: 10.2147/NDT.S264910. PMID: 33976546; PMCID: PMC8106529.

7. Guo, T., Zhang, D., Zeng, Y. et al. Molecular and cellular mechanisms underlying the pathogenesis of Alzheimer's disease. Mol Neurodegeneration 15, 40 (2020). https://doi.org/10.1186/s13024-020-00391-7

8. Sevenich Lisa,Brain-Resident Microglia and Blood-Borne Macrophages Orchestrate Central Nervous System Inflammation in Neurodegenerative Disorders and Brain Cancer, Frontiers in Immunology, Vol. 9, 2018, p 697,https://www.frontiersin.org/article/10.3389/fimmu.2018.00697, DOI=10.3389/fimmu.2018.00697, ISSN=1664-3224

9. Soscia SJ, Kirby JE, Washicosky KJ, et al. The Alzheimer's disease-associated amyloid beta-protein is an antimicrobial peptide. PLoS One. 2010;5(3):e9505. doi:10.1371/journal.pone.0009505

10. Kumar DK, Choi SH, Washicosky KJ, et al. Amyloid-β peptide protects against microbial infection in mouse and worm models of Alzheimer's disease. Sci Transl Med. 2016;8(340):340ra72. doi:10.1126/scitranslmed.aaf1059

11. Hajishengallis G, Darveau RP, Curtis MA. The keystone-pathogen hypothesis. Nat Rev Microbiol. 2012;10(10):717–725.

12. Hajishengallis G, Lamont RJ. Beyond the red complex and into more complexity: the polymicrobial synergy and dysbiosis (PSD) model of periodontal disease etiology. Mol Oral Microbiol. 2012;27(6):409–419.

13. Olsen, I., Kell, D. B., & Pretorius, E. (2020). Is Porphyromonas gingivalis involved in Parkinson's disease?. European journal of clinical microbiology & infectious diseases : official publication of the European Society of Clinical Microbiology, 39(11), 2013–2018. https://doi.org/10.1007/s10096-020-03944-2

14. Holmstrup P, Damgaard C, Olsen I, Klinge B, Flyvbjerg A, Nielsen CH, Hansen PR. Comorbidity of periodontal disease: two sides of the same coin? An introduction for the clinician. J Oral Microbiol. 2017;9(1):1332710.

15. Kozak, M., Dabrowska-Zamojcin, E., Mazurek-Mochol, M., & Pawlik, A. (2020). Cytokines and Their Genetic Polymorphisms Related to Periodontal Disease. Journal of clinical medicine, 9(12), 4045. https://doi.org/10.3390/jcm9124045

16. Forner L, Larsen T, Kilian M, Holmstrup P. Incidence of bacteremia after chewing, tooth brushing and scaling in individuals with periodontal inflammation. J Clin Periodontol. 2006 Jun;33(6):401-7. doi: 10.1111/j.1600-051X.2006.00924.x. PMID: 16677328.

17. Dominy SS, Lynch C, Ermini F, Benedyk M, Marczyk A, Konradi A, Nguyen M, Haditsch U, Raha D, Griffin C, Holsinger LJ, Arastu-Kapur S, Kaba S, Lee A, Ryder MI, Potempa B, Mydel P, Hellvard A, Adamowicz K, Hasturk H, Walker GD, Reynolds EC, Faull RLM, Curtis MA, Dragunow M, Potempa J. Porphyromonas gingivalis in Alzheimer's disease brains: Evidence for disease causation and treatment with small-molecule inhibitors. Sci Adv. 2019 Jan 23;5(1):eaau3333. doi: 10.1126/sciadv.aau3333. PMID: 30746447; PMCID: PMC6357742.

18. Poole S, Singhrao SK, Kesavalu L, Curtis MA, Crean S (2013) Determining the presence of periodontopathic virulence factors in short-term postmortem Alzheimer's disease brain tissue. J Alzheimers Dis 36, 665–677.

19. Poole S, Singhrao SK, Chukkapalli S, Rivera M, Velsko I, Kesavalu L, Crean SJ. Active invasion of Porphyromonas gingivalis and infection-induced complement activation in ApoE-/- mice brains. J Alzheimers Dis. 2015;43(1):67–80.

20. Ilievski V, Zuchowska PK, Green SJ, Toth PT, Ragozzino ME, Le K, Aljewari HW, O'Brien-Simpson NM, Reynolds EC, Watanabe K (2018) Chronic oral application of a periodontal pathogen results in brain inflammation, neurodegeneration and amyloid beta production in wild type mice. PLoS One 13, e0204941.

21 Dorn BR, Burks JN, Seifert KN, Progulske-Fox A. Invasion of endothelial and epithelial cells by strains of Porphyromonas gingivalis. FEMS Microbiol Lett. 2000;187:139–44.

22 Yoshino T, Laine ML, Van Winkelhoff AJ, Dahlén G, Genotype variation and capsular serotypes of Porphyromonas gingivalis from chronic periodontitis and periodontal abscesses, FEMS Microbiology Letters, Volume 270, Issue 1, May 2007, Pages 75–81, https://doi.org/10.1111/j.1574-6968.2007.00651.x

23 Ha JY, Choi SY, Lee JH, Hong SH, Lee HJ. Delivery of Periodontopathogenic Extracellular Vesicles to Brain Monocytes and Microglial IL-6 Promotion by RNA Cargo. Front Mol Biosci. 2020 Nov 24;7:596366. doi: 10.3389/fmolb.2020.596366. PMID: 33330627; PMCID: PMC7732644.

24 Veith PD, Chen YY, Gorasia DG, Chen D, Glew MD, O'Brien-Simpson NM, et al. Porphyromonas gingivalis outer membrane vesicles exclusively contain outer membrane and periplasmic proteins and carry a cargo enriched with virulence factors. J Proteome Res. 2014;13:2420–32. doi: 10.1021/pr401227e.

25 Abe N, Kadowaki T, Okamoto K, Nakayama K, Ohishi M, Yamamoto K. Biochemical and functional properties of lysine-specific cysteine proteinase (Lys-gingipain) as a virulence factor of Porphyromonas gingivalis in periodontal disease. J Biochem. 1998 Feb;123(2):305-12. doi: 10.1093/oxfordjournals.jbchem.a021937. PMID: 9538207.

26 Olsen, I., & Amano, A. (2015). Outer membrane vesicles - offensive weapons or good Samaritans?. Journal of oral microbiology, 7, 27468. https://doi.org/10.3402/jom.v7.27468

27 Furuta N, Takeuchi H, Amano A. Entry of Porphyromonas gingivalis outer membrane vesicles into epithelial cells causes cellular functional impairment. Infect Immun. 2009;77:4761–70. doi: 10.1128/IAI.00841-09.

28 Hajishengallis G. (2011). Immune evasion strategies of Porphyromonas gingivalis. Journal of oral biosciences, 53(3), 233–240. https://doi.org/10.2330/joralbiosci.53.233

29 Meghil, M. M., Tawfik, O. K., Elashiry, M., Rajendran, M., Arce, R. M., Fulton, D. J., Schoenlein, P. V., & Cutler, C. W. (2019). Disruption of Immune Homeostasis in Human Dendritic Cells via Regulation of Autophagy and Apoptosis by Porphyromonas gingivalis. Frontiers in immunology, 10, 2286. https://doi.org/10.3389/fimmu.2019.02286

30 Deatherage BL, Cookson BT. Membrane vesicle release in bacteria, eukaryotes, and archaea: a conserved yet underappreciated aspect of microbial life. Infect Immun. 2012;80:1948–57.

31 Nativel, B., Couret, D., Giraud, P. et al. Porphyromonas gingivalis lipopolysaccharides act exclusively through TLR4 with a resilience between mouse and human. Sci Rep 7, 15789 (2017). https://doi.org/10.1038/s41598-017-16190-y

32 Muoio V, Persson PB, Sendeski MM. The neurovascular unit - concept review. Acta Physiol (Oxf). 2014 Apr;210(4):790-8. doi: 10.1111/apha.12250. PMID: 24629161.

33 Cipolla MJ. The Cerebral Circulation. San Rafael (CA): Morgan & Claypool Life Sciences; 2009. Chapter 2, Anatomy and Ultrastructure. Available from: https://www.ncbi.nlm.nih.gov/books/NBK53086.

34 Sweeney MD, Sagare AP, Zlokovic BV. Blood-brain barrier breakdown in Alzheimer disease and other neurodegenerative disorders. Nat Rev Neurol. 2018 Mar;14(3):133-150. doi: 10.1038/nrneurol.2017.188. Epub 2018 Jan 29. PMID: 29377008; PMCID: PMC5829048.

35 Anette Wolff, Maria Antfolk, Birger Brodin, Maria Tenje, In Vitro Blood–Brain Barrier Models—An Overview of Established Models and New Microfluidic Approaches, Journal of Pharmaceutical Sciences,Volume 104, Issue 9,2015,Pages 2727-2746,ISSN 0022-3549, https://doi.org/10.1002/jps.24329.

36 Verheggen, I.C.M., de Jong, J.J.A., van Boxtel, M.P.J. et al. Increase in blood–brain barrier leakage in healthy, older adults. GeroScience 42, 1183–1193 (2020). https://doi.org/10.1007/s11357-020-00211-2

37 Lochhead Jeffrey J., Yang Junzhi, Ronaldson Patrick T., Davis Thomas P.,

Structure, Function, and Regulation of the Blood-Brain Barrier Tight Junction in Central Nervous System Disorders, Frontiers in Physiology, 11, 2020,914,

URL=https://www.frontiersin.org/article/10.3389/fphys.2020.00914 DOI=10.3389/fphys.2020.00914

38 Brown GC. The endotoxin hypothesis of neurodegeneration. J Neuroinflammation. 2019 Sep 13;16(1):180. doi: 10.1186/s12974-019-1564-7. PMID: 31519175; PMCID: PMC6744684.

39 Methia N, André P, Hafezi-Moghadam A, Economopoulos M, Thomas KL, Wagner DD. ApoE deficiency compromises the blood brain barrier especially after injury. Mol Med. 2001 Dec;7(12):810-5. PMID: 11844869; PMCID: PMC1950012.

40 Montagne, A., Nation, D.A., Sagare, A.P. et al. APOE4 leads to blood–brain barrier dysfunction predicting cognitive decline. Nature 581, 71–76 (2020). https://doi.org/10.1038/s41586-020-2247-3

41 Dando SJ, Mackay-Sim A, Norton R, et al. Pathogens penetrating the central nervous system: infection pathways and the cellular and molecular mechanisms of invasion. Clin Microbiol Rev. 2014;27(4):691–726. doi:10.1128/CMR.00118-13

42 Coureuil M, Lécuyer H, Bourdoulous S, Nassif X. A journey into the brain: insight into how bacterial pathogens cross blood-brain barriers. Nat Rev Microbiol. 2017 Mar;15(3):149-159. doi: 10.1038/nrmicro.2016.178. Epub 2017 Jan 16. PMID: 28090076.

43 Takeuchi, H., Sasaki, N., Yamaga, S., Kuboniwa, M., Matsusaki, M., & Amano, A. (2019). Porphyromonas gingivalis induces penetration of lipopolysaccharide and peptidoglycan through the gingival epithelium via degradation of junctional adhesion molecule 1. PLoS pathogens, 15(11), e1008124. https://doi.org/10.1371/journal.ppat.1008124

44 Sheets, S. M., Potempa, J., Travis, J., Casiano, C. A., & Fletcher, H. M. (2005). Gingipains from Porphyromonas gingivalis W83 induce cell adhesion molecule cleavage and apoptosis in endothelial cells. Infection and immunity, 73(3), 1543–1552. https://doi.org/10.1128/IAI.73.3.1543-1552.2005

45 Yuhan He, Noriko Shiotsu, Yoko Uchida-Fukuhara, Jiajie Guo, Yao Weng, Mika Ikegame, Ziyi Wang, Kisho Ono, Hiroshi Kamioka, Yasuhiro Torii, Akira Sasaki, Kaya Yoshida, Hirohiko Okamura, Outer membrane vesicles derived from Porphyromonas gingivalis induced cell death with disruption of tight junctions in human lung epithelial cells, Archives of Oral Biology, Volume 118, 2020, 104841, ISSN 0003-9969, https://doi.org/10.1016/j.archoralbio.2020.104841.

46 Solleiro-Villavicencio H, Rivas-Arancibia S, Effect of Chronic Oxidative Stress on Neuroinflammatory Response Mediated by CD4+T Cells in Neurodegenerative Diseases, Frontiers in Cellular Neuroscience, 12, 2018,114
URL=https://www.frontiersin.org/article/10.3389/fncel.2018.00114

DOI=10.3389/fncel.2018.00114

47 Banks, W.A., Gray, A.M., Erickson, M.A. et al. Lipopolysaccharide-induced blood-brain barrier disruption: roles of cyclooxygenase, oxidative stress, neuroinflammation, and elements of the neurovascular unit. J Neuroinflammation 12, 223 (2015). https://doi.org/10.1186/s12974-015-0434-1

48 Wang, X., Xue, G.-X., Liu, W.-C., Shu, H., Wang, M., Sun, Y., Liu, X., Sun, Y.E., Liu, C.-F., Liu, J., Liu, W. and Jin, X. (2017), Melatonin alleviates lipopolysaccharide-compromised integrity of blood–brain barrier through activating AMP-activated protein kinase in old mice. Aging Cell, 16: 414-421. https://doi.org/10.1111/acel.12572

49 Pflanzner T, Kuhlmann CR, Pietrzik CU. Blood-brain-barrier models for the investigation of transporter- and receptor-mediated amyloid-β clearance in Alzheimer's disease. Curr Alzheimer Res. 2010 Nov;7(7):578-90. doi: 10.2174/156720510793499066. PMID: 20704558.

50 Kumar, S., Shaw, L., Lawrence, C., Lea, R. and Alder, J. (2014) 'P50 * Developing a Physiologically Relevant Blood Brain Barrier Model for the Study of Drug Disposition in Glioma', Neuro-Oncology, 16(suppl 6), p. vi8-vi8. doi: 10.1093/neuonc/nou249.38

51 Hughes, P., Marshall, D., Reid, Y., Parkes, H. & Gelber, C. (2007). The costs of using unauthenticated, over-passaged cell lines: how much more data do we need? Biotechniques, 43, 575, 577-8, 581-2

52 Srinivasan, B., Kolli, A. R., Esch, M. B., Abaci, H. E., Shuler, M. L., & Hickman, J. J. (2015). TEER measurement techniques for in vitro barrier model systems. Journal of laboratory automation, 20(2), 107–126. https://doi.org/10.1177/2211068214561025

53 Zwain, Tamara Akeel abdulmunim, Alder, Jane Elizabeth , Sabagh, Bassem, Shaw, Andrew, Burrow, Andrea Julie and Singh, Kamalinder (2021) Tailoring functional nanostructured lipid carriers for glioblastoma treatment with enhanced permeability through in-vitro 3D BBB/BBTB models. Materials Science and Engineering: C, 121 (111774). ISSN 0928-4931

54 Seyama M, Yoshida K, Yoshida K, Fujiwara N, Ono K, Eguchi T, Kawai H, Guo J, Weng Y, Haoze Y, Uchibe K, Ikegame M, Sasaki A, Nagatsuka H, Okamoto K, Okamura H, Ozaki K. Outer membrane vesicles of Porphyromonas gingivalis attenuate insulin sensitivity by delivering gingipains to the liver. Biochim Biophys Acta Mol Basis Dis. 2020 Jun 1;1866(6):165731. doi: 10.1016/j.bbadis.2020.165731. Epub 2020 Feb 20. PMID: 32088316.

55 Danaei M, Dehghankhold M, Ataei S, Hasanzadeh Davarani F, Javanmard R, Dokhani A, Khorasani S, Mozafari MR. Impact of Particle Size and Polydispersity Index on the Clinical Applications of Lipidic Nanocarrier Systems. Pharmaceutics. 2018 May 18;10(2):57. doi: 10.3390/pharmaceutics10020057. PMID: 29783687; PMCID: PMC6027495.

56 Helms HC, Abbott NJ, Burek M, Cecchelli R, Couraud PO, Deli MA, Förster C, Galla HJ, Romero IA, Shusta EV, Stebbins MJ, Vandenhaute E, Weksler B, Brodin B. In vitro models of the blood-brain barrier: An overview of commonly used brain endothelial cell culture models and guidelines for their use. J Cereb Blood Flow Metab. 2016 May;36(5):862-90. doi: 10.1177/0271678X16630991. Epub 2016 Feb 11. PMID: 26868179; PMCID: PMC4853841.

57 Iarosh OA. Matematicheskiĭ analiz pronitsaemosti gematoéntsefalicheskogo ber'era pri bakterial'nom meningoéntsefalite [Mathematical analysis of permeability of the blood-brain barrier in bacterial meningoencephalitis]. Zh Nevropatol Psikhiatr Im S S Korsakova. 1992;92(2):33-6. Russian. PMID: 1326169.

58. Kanoh Y, Ohara T, Akahoshi T. Acute inflammatory biomarkers in cerebrospinal fluid as indicators of blood cerebrospinal fluid barrier damage in Japanese subjects with infectious meningitis. Clin Lab. 2011;57(1-2):37-46. PMID: 21391463.

59 Blufstein, A, Behm, C, Nguyen, PQ, Rausch-Fan, X, Andrukhov, O. Human periodontal ligament cells exhibit no endotoxin tolerance upon stimulation with Porphyromonas gingivalis lipopolysaccharide. J Periodont Res. 2018; 53: 589– 597. https://doi.org/10.1111/jre.12549

60 Hirasawa, M., & Kurita-Ochiai, T. (2018). Porphyromonas gingivalis Induces Apoptosis and Autophagy via ER Stress in Human Umbilical Vein Endothelial Cells. Mediators of inflammation, 2018, 1967506. https://doi.org/10.1155/2018/1967506

61 Wilhelm I, Fazakas C and Krizbai I A, In vitro models of the blood-brain barrier, Acta Neurobiol Exp 2011, 71: 113–128

62 Hoffmann, A., Bredno, J., Wendland, M., Derugin, N., Ohara, P., & Wintermark, M. (2011). High and Low Molecular Weight Fluorescein Isothiocyanate (FITC)-Dextrans to Assess Blood-Brain Barrier Disruption: Technical Considerations. Translational stroke research, 2(1), 106–111. https://doi.org/10.1007/s12975-010-0049-x

63 Fabry Z, Fitzsimmons KM, Herlein JA, Moninger TO, Dobbs MB, Hart MN. Production of the cytokines interleukin 1 and 6 by murine brain microvessel endothelium and smooth muscle pericytes. J Neuroimmunol. 1993 Aug;47(1):23-34. doi: 10.1016/0165-5728(93)90281-3. PMID: 8376546.

64 Behm C, Blufstein A, Abhari SY, Koch C, Gahn J, Schäffer C, Moritz A, Rausch-Fan X, Andrukhov O. Response of Human Mesenchymal Stromal Cells from Periodontal Tissue to LPS Depends on the Purity but Not on the LPS Source. Mediators Inflamm. 2020 Jul 2;2020:8704896. doi: 10.1155/2020/8704896. PMID: 32714091; PMCID: PMC7352132.

65 Olsen, I., & Progulske-Fox, A. (2015). Invasion of Porphyromonas gingivalis strains into vascular cells and tissue. Journal of oral microbiology, 7, 28788. https://doi.org/10.3402/jom.v7.28788

66 Coats, S. R., Kantrong, N., To, T. T., Jain, S., Genco, C. A., McLean, J. S., & Darveau, R. P. (2019). The Distinct Immune-Stimulatory Capacities of Porphyromonas gingivalis Strains 381 and ATCC 33277 Are Determined by the fimB Allele and Gingipain Activity. Infection and immunity, 87(12), e00319-19. https://doi.org/10.1128/IAI.00319-19

67 Bergmann, S., Lawler, S. E., Qu, Y., Fadzen, C. M., Wolfe, J. M., Regan, M. S., Pentelute, B. L., Agar, N., & Cho, C. F. (2018). Blood-brain-barrier organoids for investigating the permeability of CNS therapeutics. Nature protocols, 13(12), 2827–2843. https://doi.org/10.1038/s41596-018-0066-x

68 Nádházi Z, Takáts A, Offenmüller K, Bertók L. Plasma endotoxin level of healthy donors. Acta Microbiol Immunol Hung. 2002;49:151–157. doi: 10.1556/AMicr.49.2002.1.15.

69 Kalash D, Vovk A, Huang H, Aukhil I, Wallet SM, Shaddox LM. Influence of periodontal therapy on systemic lipopolysaccharides in children with localized aggressive periodontitis. Pediatr Dent. 2015;37:35–40.

70 Wahaidi VY, Kowolik MJ, Eckert GJ, Galli DM. Endotoxemia and the host systemic response during experimental gingivitis. J Clin Periodontol. 2011;38:412–417. doi: 10.1111/j.1600-051X.2011.01710.x.

71 Zhang R, Miller RG, Gascon R, et al. Circulating endotoxin and systemic immune activation in sporadic amyotrophic lateral sclerosis (sALS) J Neuroimmunol. 2009;206:121–124. doi: 10.1016/j.jneuroim.2008.09.017.

72 Zhao Y, Jaber V, Lukiw WJ. Secretory products of the human GI tract microbiome and their potential impact on Alzheimer's disease (AD): detection of lipopolysaccharide (LPS) in AD hippocampus. Front Cell Infect Microbiol. 2017;7:318. doi: 10.3389/fcimb.2017.00318.

73 Vargas-Caraveo, A., Sayd, A., Maus, S.R. et al. Lipopolysaccharide enters the rat brain by a lipoprotein-mediated transport mechanism in physiological conditions. Sci Rep 7, 13113 (2017). https://doi.org/10.1038/s41598-017-13302-6

74 Jaeger LB, Dohgu S, Sultana R, et al. Lipopolysaccharide alters the blood–brain barrier transport of amyloid β protein: a mechanism for inflammation in the progression of Alzheimer's disease. Brain Behav Immun. 2009;23:507–517. doi: 10.1016/j.bbi.2009.01.017.

75 Bryant CE, Spring DR, Gangloff M, et al. The molecular basis of the host response to lipopolysaccharide. Nat Rev Microbiol. 2010;8:8–14. doi: 10.1038/nrmicro2266.

76 Morris MC, Gilliam EA, Li L. Innate immune programing by endotoxin and its pathological consequences. Front Immunol. 2015;5:680. doi: 10.3389/fimmu.2014.00680.

77 Wendeln AC, Degenhardt K, Kaurani L, Gertig M, Ulas T, Jain G, Wagner J, Häsler LM, Wild K, Skodras A, Blank T, Staszewski O, Datta M, Centeno TP, Capece V, Islam MR, Kerimoglu C, Staufenbiel M, Schultze JL, Beyer M, Prinz M, Jucker M, Fischer A, Neher JJ. Innate immune memory in the brain shapes neurological disease hallmarks. Nature. 2018;556:332–338. doi: 10.1038/s41586-018-0023-4.

78 Sandiego CM, Gallezot JD, Pittman B, Nabulsi N, Lim K, Lin SF, Matuskey D, Lee JY, O'Connor KC, Huang Y, Carson RE, Hannestad J, Cosgrove KP. Imaging robust microglial activation after lipopolysaccharide administration in humans with PET. Proc Natl Acad Sci U S A. 2015;112:12468–12473. doi: 10.1073/pnas.1511003112.

79 Skelly DT, Hennessy E, Dansereau MA, Cunningham C. A systematic analysis of the peripheral and CNS effects of systemic LPS, IL-1β, TNF-α and IL-6 challenges in C57BL/6 mice. PLoS One. 2013;8:e69123. doi: 10.1371/journal.pone.0069123.

80. Eigenmann DE, Xue G, Kim KS, Moses AV, Hamburger M, Oufir M. Comparative study of four immortalized human brain capillary endothelial cell lines, hCMEC/D3, hBMEC, TY10, and BB19, and optimization of culture conditions, for an in vitro blood-brain barrier model for drug permeability studies. Fluids Barriers CNS. 2013 Nov 22;10(1):33. doi: 10.1186/2045-8118-10-33. PMID: 24262108; PMCID: PMC4176484.

81 Belardi B, Hamkins-Indik T, Harris AR, Kim J, Xu K, Fletcher DA. A Weak Link with Actin Organizes Tight Junctions to Control Epithelial Permeability. Dev Cell. 2020 Sep 28;54(6):792-804.e7. doi: 10.1016/j.devcel.2020.07.022. Epub 2020 Aug 24. PMID: 32841596; PMCID: PMC7530003.

82 Tornavaca, O., Chia, M., Dufton, N., Almagro, L. O., Conway, D. E., Randi, A. M., Schwartz, M. A., Matter, K., & Balda, M. S. (2015). ZO-1 controls endothelial adherens junctions, cell-cell tension, angiogenesis, and barrier formation. The Journal of cell biology, 208(6), 821–838. https://doi.org/10.1083/jcb.201404140

83 Stamatovic, S. M., Johnson, A. M., Keep, R. F., & Andjelkovic, A. V. (2016). Junctional proteins of the blood-brain barrier: New insights into function and dysfunction. Tissue barriers, 4(1), e1154641. https://doi.org/10.1080/21688370.2016.1154641